AD-A257 738

NAVAL POSTGRADUATE SCHOOL
Monterey, California

THESIS

THE DEFORMATION CHARACTERISTICS AND
MICROSTRUCTURAL DYNAMICS
OF AN AL-10MG-0.1ZR ALLOY

by

James F. Buckley II

June 1992

Thesis Advisor   T.R. McNelley

92-30734

Unclassified

security classification of this page

REPORT DOCUMENTATION PAGE

1a Report Security Classification Unclassified		1b Restrictive Markings		
2a Security Classification Authority		3 Distribution Availability of Report		
2b Declassification Downgrading Schedule		Approved for public release; distribution is unlimited.		
4 Performing Organization Report Number(s)		5 Monitoring Organization Report Number(s)		
6a Name of Performing Organization Naval Postgraduate School	6b Office Symbol (if applicable) 34	7a Name of Monitoring Organization Naval Postgraduate School		
6c Address (city, state, and ZIP code) Monterey, CA 93943-5000		7b Address (city, state, and ZIP code) Monterey, CA 93943-5000		
8a Name of Funding Sponsoring Organization	8b Office Symbol (if applicable)	9 Procurement Instrument Identification Number		
8c Address (city, state, and ZIP code)		10 Source of Funding Numbers		
		Program Element No	Project No	Task No	Work Unit Accession No

11 Title (include security classification) THE DEFORMATION CHARACTERISTICS AND MICROSTRUCTURAL DYNAMICS OF AN Al-10MG-0.1ZR ALLOY

12 Personal Author(s) James F. Buckley II

13a Type of Report Master's Thesis	13b Time Covered From To	14 Date of Report (year, month, day) June 1992	15 Page Count 63

16 Supplementary Notation The views expressed in this thesis are those of the author and do not reflect the official policy or position of the Department of Defense or the U.S. Government.

17 Cosati Codes			18 Subject Terms (continue on reverse if necessary and identify by block number)
Field	Group	Subgroup	word processing, Script, GML, text processing.

19 Abstract (continue on reverse if necessary and identify by block number)

An investigation into microstructural evolution during processing and superplastic deformation of an Al-10Mg-0.1Zr alloy was conducted. Processing schedules were modified to enhance particle-stimulated nucleation of recrystallization and refine subsequent grain size. Strain rates varying over three orders of magnitude were utilized in subsequent testing of processed material. At lower strain rates of about 10^{-4} sec^{-1} coarsening of the microstructure was apparent and elongations of 277% were obtained. A strain rate of 10^{-3} sec^{-1} resulted in lesser coarsening and elongations of 650%. A model of deformation by grain boundary sliding in association with microstructural coarsening is presented.

20 Distribution Availability of Abstract ☒ unclassified unlimited ☐ same as report ☐ DTIC users	21 Abstract Security Classification Unclassified	
22a Name of Responsible Individual T.R. McNelley	22b Telephone (include Area code) (408) 646-2589	22c Office Symbol ME Mc

DD FORM 1473,84 MAR   83 APR edition may be used until exhausted   security classification of this page
All other editions are obsolete

Unclassified

i

The Deformation Characteristics and Microstructural Dynamics
of an Al-10Mg-0.1Zr Alloy

by

James F. Buckley II
Lieutenant, United States Navy
B.S., Cornell University, 1985

Submitted in partial fulfillment of the
requirements for the degree of

MASTER OF SCIENCE IN MECHANICAL ENGINEERING
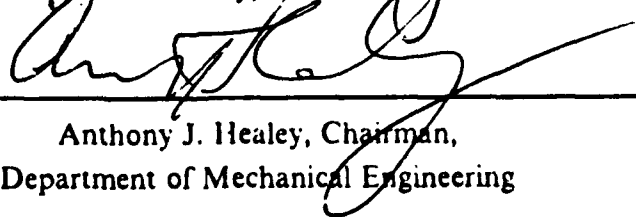
from the

NAVAL POSTGRADUATE SCHOOL
June 1992

Author: _____

James F. Buckley II

Approved by: _____

T.R. McNelley, Thesis Advisor

_____

Anthony J. Healey, Chairman,
Department of Mechanical Engineering

ii

ABSTRACT

An investigation into microstructural evolution during processing and superplastic deformation of an Al-10Mg-0.1Zr alloy was conducted. Processing schedules were modified to enhance particle-stimulated nucleation of recrystallization and refine subsequent grain size. Strain rates varying over three orders of magnitude were utilized in subsequent testing of processed material. At lower strain rates of about 10^{-4} sec^{-1} coarsening of the microstructure was apparent and elongations of 277% were obtained. A strain rate of 10^{-3} sec^{-1} resulted in lesser coarsening and elongations of 650%. A model of deformation by grain boundary sliding in association with microstructural coarsening is presented.

DTIC QUALITY INSPECTED 2

iii

TABLE OF CONTENTS

LIST OF TABLES

LIST OF FIGURES

I. INTRODUCTION

The phenomenon of superplasticity has been known for many years, but only in the last twenty years have materials and processes been developed which are commercially usable. Several metallic alloys and even some ceramics are capable of superplastic deformation. Superplasticity is the ability to sustain large tensile deformation, i.e. greater than 200%, of some polycrystalline metallic materials [Ref. 1: p.358]. This phenomenon was first seen as early as 1912 when Bengough [Ref. 2] observed that certain types of α β brass exhibited elongations of 200% and necked to a fine point. That work also referred to observations regarding viscous-like behavior in some fine-grained alloys such as Pb-Sn alloys which are low-strength non-structural materials [Ref. 1: p.359].

Work done in the former Soviet Union in this area was reviewed by Underwood [Ref. 3] in 1962 and this rekindled interest in the West. The result has been the development of superplastic response in Titanium alloys, steels and Aluminum alloys, all of potential commercial use. Even some ceramics are now known to be capable of superplastic deformation [Ref. 4,5]. For many of these materials either the strength is too low or the forming temperature too high to be of current practical use.

Several Aluminum alloys are found to be capable of superplastic deformation provided the appropriate stages of thermomechanical processing are carefully controlled. Aluminum alloys are especially desirable because of their high strength-to-weight ratio, corrosion resistance, and low cost. In recent years, research on Al-Mg alloys has provided materials which are capable of superplastic deformation at 300°C, the same used in processing and a temperature below the Mg solvus for the alloy. Further, deforming forces are comparable to higher temperature superplastic aluminum alloys provided the strain rates are also kept low [Ref. 6: p.33].

1

Capacity for plastic flow is generally associated with three mechanisms: one, slip by dislocation movement; two, grain boundary sliding of adjacent grains; and three, stress-directed diffusion [Ref. 1: p.355]. A common characteristic of superplastic materials is a fine, recrystallized grain size stabilized by second phase particles. A fine grain size facilitates deformation by grain boundary sliding during deformation at elevated temperatures. Also, the grain boundaries must have low atomic registry, i.e., grain boundaries, should be of high misorientation angle in order for grain boundary sliding to occur.

For Al-Mg alloys of this research, the second-phase particles are the β phase (Al_8Mg_5). The roles of such second phase particles in processing and superplastic deformation are not completely understood. Sufficiently fine particles ($\ll 1.0\mu m$) may retard boundary migration and thus aid in achieving a fine grain size, while coarser particles ($> 1.0\mu m$) may serve as nucleation sites for recrystallization during the processing. The microstructural effects of intermediate-sized particles have not been completely characterized.

Manufacturing by means of superplastic forming has in recent years become an industrially recognized means for producing parts. One of the leaders in this field is the aircraft industry. The strength-to-weight ratio advantages of Aluminum alloys are enhanced by further weight reduction brought about due to elimination of the need for fasteners when manufacturing parts using superplastic forming. By forming complex and intricate parts in this manner, joint wear and corrosion are also reduced. An example of such an application is the construction of aircraft wing and rudder struts [Ref. 7: pp.51-52]. When these parts are superplastically formed they may be readily finished such that the surface is highly smooth and easily lubricated thus reducing wear. Also, when parts or assemblies are superplastically formed some conventional manufacturing steps may be eliminated thereby reducing production costs. By using superplastic forming techniques, complex parts may be manufactured with minimal deforming

2

forces and energy consumption. Further, the resulting fine grained microstructure and uniform material properties throughout the material may prove beneficial during the service life of the part.

The purpose of this research is an attempt improve the superplastic properties of the Al-10Mg-0.1Zr alloy by modifying the thermomechanical processing schedule developed in previous work at the Naval Postgraduate School. By modifying this schedule to achieve particle stimulated nucleation of recrystallization at finer particles the microstructure produced will be finer in grain size and capable of greater superplastic ductility.

II. BACKGROUND

A. ALUMINUM ALLOYS-GENERAL

Aluminum ranks second only to steel and iron in volume and weight consumed industrially each year. Aluminum-Magnesium alloys account for nearly half of the total annual aluminum production as measured by volume [Ref. 8]. Development and improvement of processing techniques for these alloys could have potentially far reaching effects. Aluminum alloys are used widely for many consumer products, extensively in the aerospace industry and increasingly by the automotive industry. High strength-to-weight ratio, low-density, high-ductility alloys provide components which are both strong and light weight which translates to fuel savings.

Strengthening of Aluminum alloys is commonly achieved through a combination of solid solution and strain hardening mechanisms for non-heat treatable alloys, and by precipitation and dispersion strengthening for those which may be heat treated. Solid solution strengthening occurs [Ref. 9] when misfitting solute atoms are introduced into the lattice to impede dislocation motion by interacting with the distortion field of the dislocations. If the material is then deformed the dislocation density will increase. Dislocation-dislocation interaction will act additively to further strengthen the material. A pure metal would contain no solute atoms and dislocations would travel more freely through the structure imparting little strength and allowing for ease of deformation.

Precipitation and dispersion strengthening are similar in nature in that, for both cases, fine particles which are relatively hard compared to the matrix material are distributed throughout the material. This occurs either by precipitation upon cooling or by disbursal throughout the matrix by other means. These small hard particles will impede dislocation movement and strengthen the material [Ref. 10]. Precipitation harden-

ing is accomplished through a three-step process of solution treatment followed by quenching and then aging of the material.

The most widely used of the Aluminum alloys are those based on the Aluminum-Magnesium system [Ref. 8]. Magnesium is added to aluminum to provide solid solution strengthening. The resulting alloys are of moderate strength, good corrosion resistance and also are weldable. When the alloys of sufficient Mg content are cooled from a supersaturated solution, the β phase precipitates out. In general these β particles are too large and widely spaced to strengthen via the precipitation or dispersion mechanisms. However, the size and distribution of these β particles will affect the grain size and the superplastic properties of the alloy by their influence on recrystallization. This will be the focus of the current research.

B. MICROSTRUCTURAL PREREQUISITES FOR SUPERPLASTIC FLOW

Grains below $5\text{-}10\mu m$ in size are required to support superplastic deformation. Superplastic behavior is never observed in single phase materials due to rapid grain growth upon heating [Ref. 1: p.367]. The size of the grains must be maintained by the presence of a second phase in the microstructure. In the case of Aluminum-Magnesium (Al-Mg) alloys this will be the β phase (Mg_5Al_8). This secondary phase inhibits grain growth when the material is heated thereby providing the stability at elevated temperatures required for superplastic flow. This requirement for a second phase is why most superplastic materials are based on either eutectic, eutectoid, or monotectoid alloy systems [Ref. 1: p.369].

The second phase may also contribute to the strength of the alloy at ordinary temperatures. If the second phase is hard compared to the matrix material, cavitation may result upon straining. To prevent this cavitation, the strengths of the primary and secondary phases should be close to one another and the particles evenly spaced. In the

5

case of the Al-Mg alloys, the β phase particles are hard at low temperatures but soften at elevated temperatures of $0.5 - 0.6T_m$.

The misorientation angle between grains must be high. $\theta > 15^c$ [Ref. 11], as the primary mechanism of deformation during superplastic flow is grain boundary sliding. Grains with low angle boundaries will not support grain boundary sliding do to a high degree of atomic registry. High atomic registry prevents the grains from sliding with respect to one another in the presence of shear stress. The required high angle grain boundaries are readily formed by processing of the Al-Mg material at intermediate temperatures. Further, the grain boundaries must also be mobile so they are able to alleviate stress concentrations which develop at grain boundary triple points in the matrix. High boundary mobility is reflected in the observation that grains remain equiaxed and stable during superplastic deformation.

C. ALUMINUM-MAGNESIUM ALLOYS

As mentioned earlier. Al-Mg alloys are used quite extensively in industry. The strength-to-weight ratio combined with their formability, weldability and corrosion resistance make such alloys very attractive for a wide range of commercial and military applications including aerospace uses. As seen in Figure 1, Mg is highly soluble in Al, up to $\approx 15\%$ at the eutectic temperature ($451°C$). As the temperature is reduced the Mg solubility decreases and β phase particle maybe precipitated out of solution. The solvus temperature for alloys of interest here (containing 10 pct. Mg) is $\approx 365°C$.

Early work on Al-Mg alloys at the Naval Postgraduate School focused on processing techniques to control the size and distribution of these second phase β particles. The β phase tends to form preferentially on grain boundaries unless processing is devised to provide a more homogenous distribution. Once located on the grain boundaries, the β particles facilitate initiation of stress corrosion cracking in a marine environments. If a processing schedule could be developed which would disperse the β phase particles
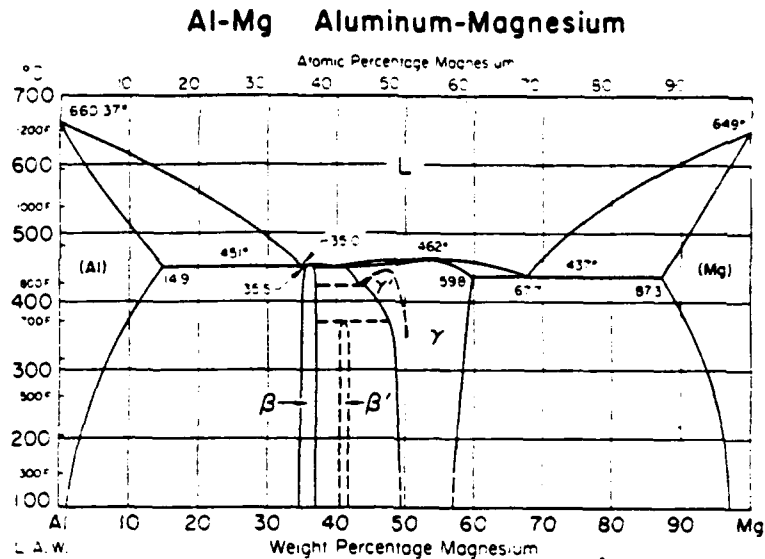
Al-Mg   Aluminum-Magnesium

Figure 1.   Aluminum-Magnesium Phase Diagram [Ref. 8]

throughout the matrix during processing, the subsequent susceptibility to stress corro-
sion cracking would be greatly decreased. Because Aluminum is a high stacking-fault
energy material, only recovery without recrystallization is expected at intermediate
processing temperatures. Hence, strength should not be greatly decreased.

A thermomechanical processing (TMP) schedule was developed to achieve the such
control of β particle distribution and size. The TMP consisted of a series of warm rolling
passes with accompanying interpass anneals at T = 300°C. Following processing these
materials were examined via transmission electron microscopy. The β phase particles
were seen to be uniformly distributed throughout the microstructure. However, the
microstructure also appeared to have recrystallized to a fine grain size yet processing
temperatures were well below those normally associated with recrystallization in such

7

materials. When samples were pulled to failure in elevated temperature tensile tests at 300°C, large elongations were obtained indicating deformation by superplastic flow [Ref. 12].

Initially it was believed [Ref. 13: p.1046] that recrystallization was occurring by a continuous recrystallization reaction (CRX) during the anneal period between rolling passes. The second-phase particles were thought to be stabilizing the structure. It was proposed that as the dislocations due to deformation merged with particle-stabilized sub-boundaries, the dislocation spacing decreased causing an increase in the misorientation angle of the boundaries. When, after sufficient cycles of deformation and annealing the misorientation angle became great enough, a new grain was formed and the material became recrystallized.

Later work by Crooks, Kalu, and McNelley [Ref. 14] focused in more detail on the role of the β particles during recrystallization. By studying the microstructure of the processed material using backscattered electron imaging in the scanning electron micro-scope they were able to show evidence of recrystallization by particle stimulated nucleation [Ref. 14: p. 1322]. During deformation sufficiently large particles become sources for dislocation arrays which constitute deformation zones. If the particle is of a size greater then a critical value, the resultant deformation zone may serve as a nucleation site for recrystallization. The critical particle size, d_{crit}, is the smallest size particle capable of inducing a deformation zone which will support PSN. The recrys-tallized grain size is inversely related to the number of particles acting as active nucleation sites for PSN. Critical particle size is an inverse function of the strain as shown in Figure 2, and therefore may be regulated by TMP selection. In this work, it is assumed that the strain is the strain per pass in the final stage of the TMP. Low strains result in fewer active nucleation sites and a coarser microstructure which will not support superplastic deformation. A high strain process produces a large number of

8

active nucleation sites resulting in a finer grain structure. Particles which are below the critical particle size for nucleation will serve to impede grain growth thereby stabilizing the microstructure at elevated temperatures.

D. PHENOMENOLOGICAL EQUATIONS FOR SUPERPLASTICITY

Three factors which are of great influence on superplastic response are temperature, grain size, and deformation rate [Ref. 1: pp.370-371]. Diffusional processes are necessary for accommodation of grain boundary sliding. Also, fine grain size facilitates grain boundary sliding along with and diffusional accommodation of the process. Hence, the constitutive equations for superplastic deformation take the form:

$$\dot{\varepsilon}_{spd} = AD_{eff}(\frac{1}{d^p})(\frac{\sigma}{E})^n \tag{1}$$

where $\dot{\varepsilon}_{spd}$ is the deformation strain rate, A is a material constant, D_{eff} is the effective diffusion coefficient, d is the grain size, p is the grain size exponent, σ is the applied stress, E is Young's modulus, and n is stress exponent. The stress exponent is inversely related to the strain rate sensitivity coefficient m. The strain rate sensitivity coefficient, m, is given by:

$$m = \frac{\partial \ln \sigma}{\partial \ln \dot{\varepsilon}} \tag{2}$$

and $m = \frac{1}{n}$ if temperature and grain size are held fixed. In general, as the m-value increases resistance to localized necking increases thereby enhancing ductility.

By examining eqn(1) it may be seen that, for a given applied stress and deformation temperature, an increase in the grain size will reduce the strain rate for superplastic deformation. Typically, highly superplastic materials have m-values of about 0.5. These materials also tend to have a relationship between strain rate and grain size given by $\dot{\varepsilon} \propto \frac{1}{d^2}$. Using this relationship and an m-value of 0.5, eqn(1) becomes:
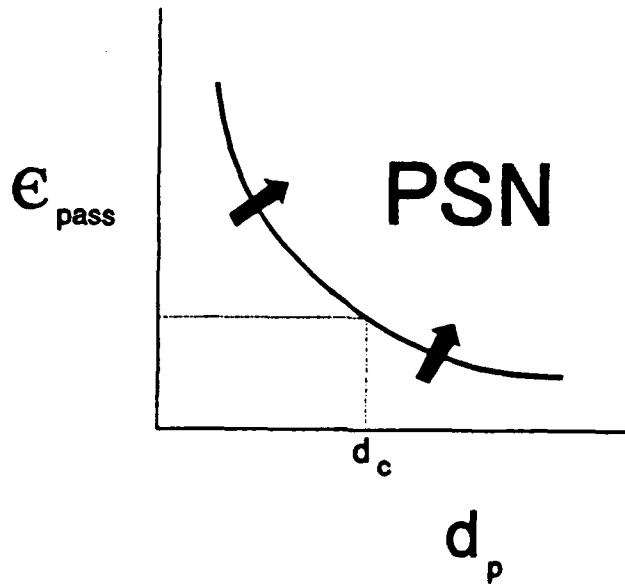
Figure 2. Relationship Between Strain and Critical Particle Size

$$\dot{\varepsilon}_{spd} = (\frac{A \, D_{eff}}{d^2})(\frac{\sigma}{E})^{\frac{1}{2}}$$ (3)

This form of the equation has been shown to be applicable to this Al-10mg-0.1Zr alloy [Ref. 15: pp.45-55]

Hamilton, Ash, Sherwood, and Heikkinen [Ref. 16; p.50] and others have examined grain growth during superplastic flow and found grain size to be both a function strain, strain rate and time at temperature. As such, the grain size $d = d(\varepsilon, \dot{\varepsilon})$ during straining. Combining this with equations (2) and (3), an apparent strain rate sensitivity coefficient, m_{app}, may be calculated as:

$$m_{app} = \frac{1}{2} + [\frac{\partial \ln d(\varepsilon, \dot{\varepsilon})}{\partial \ln \dot{\varepsilon}}]$$ (4)

The apparent strain rate sensitivity coefficient is that which is measured when grain growth is taken into account. Generally, grain growth during straining is more rapid at lower strain rates, i.e., is greater with strain at lower strain rates, and the second term on the right side of eqn(4) is negative. Eqn(4) shows that a material whose grain size coarsens during deformation will experience a reduction in apparent m-value. This reduction in m-value will in turn increase the materials susceptibility to localized necking, which decreases ductility. The reduction in ductility in the coarser grained material is consistent with a coarser microstructure not supporting as readily deformation by grain boundary sliding. Equations (1) and (3) also indicate that grain growth will result in apparent strain hardening in that the stress increase to maintain strain rate if d increases. This may aid the ductility [Ref. 16], although eventually grain growth will suppress grain boundary sliding and result in dislocation deformation mechanisms. Coarsening of the grains during processing or deformation takes place because of an unstable microstructure. Thus if a material's recrystallized microstructure is unstable, superplastic response may be degraded despite initially being in the superplastic regime.

E. TMP MODIFICATION

By manipulating the thermomechanical processing variables, namely strain per pass, number of passes, total strain, and annealing time between passes the microstructure and properties of the alloy may be changed. In an attempt to increase microstructural stability and enhance superplastic properties of this Al-Mg alloy, Gorsuch developed a processing schedule designated TMP6 [Ref.17: pp. 20-42]. This schedule consisted of a series of 12 warm rolling passes with increasing strain on successive passes coupled with 30 minute interpass anneals at 300°C. The microstructure which resulted from TMP6 consisted of homogeneously distributed β phase particles 1-2μm in size and a recrystallized microstructure. When pulled to failure in elevated temperature tensile tests conducted over a range of strain rates, elongations of greater then 1100% were achieved.

11

The PSN model assumes site saturation of all active nucleation sites at time $t = 0$ and grain growth only to the point that the nucleated grains impinge. Thus, if the density of the active nucleation sites is increased the spacing between sites will decrease and the resulting recrystallized grain size will be smaller. According to the phenomenological model presented earlier, this would increase the strain rates over which the material would deform superplastically.

The required increase in active nucleation sites for this to may be accomplished by decreasing the critical particle size for nucleation. The relationship between critical particle size and strain was shown in Figure 2. By increasing the amount of strain the material experiences in a pass, the critical particle size for nucleation will be decreased. Using this concept, the TMP6 schedule was modified to provide more strain in the final rolling pass while maintaining the same total strain. The aim of this modification was to reduce the critical particle size required for nucleation thereby obtaining a finer recrystallized microstructure capable of sustaining greater superplastic deformation.

III. EXPERIMENTAL PROCEDURE

A. MATERIAL

A direct-chill cast ingot 6.0 in (152 mm) in diameter designated, #S572826, was provided by the Alcoa Technical Center, Alcoa Center, Pennsylvania and had a nominal composition of Al-10Mg-0.1Zr wt% [Ref. 18 : p.14]. The complete chemical composition is shown in Table 1

Table 1. NOMINAL ALLOY COMPOSITION (WT%).

Casting	Mg	Zr	Si	Fe	Ti	Be	Al
S572826	9.89	0.09	0.02	0.02	0.01	0.003	Balance

The ingot was sectioned into billets such that the greatest dimension was parallel to the ingot longitudinal direction. The resultant billets had dimensions of 3.75in x 1.25 in x 1.25in (93.5mm x 31.8mm x 31.8mm) [Ref. 18 : pp. 14-22].

B. THERMOMECHANICAL PROCESSING

Thermomechanical processing (TMP) of the material was conducted in two phases the general scheme for which is shown in Figure 3. Phase one of this process was completed prior to this research in work done by Lyle [Ref. 18: p. 14]. The billets were homogenized in a Lindburg furnace for 6 hours at a temperature of 440°C. Solid solution treatment followed for 18 hours at 480°C.

The billets were then upset forged along the longitudinal direction to a thickness of 1.0 inches (25.4 mm) +/- 0.05 inches (0.1 mm) using a Baldwin-Tate-Emery testing machine equipped with the platens preheated to 440°C. Upset forging was followed by a one-hour resolution treatment at 480°C to ensure all subsequent quenching was done
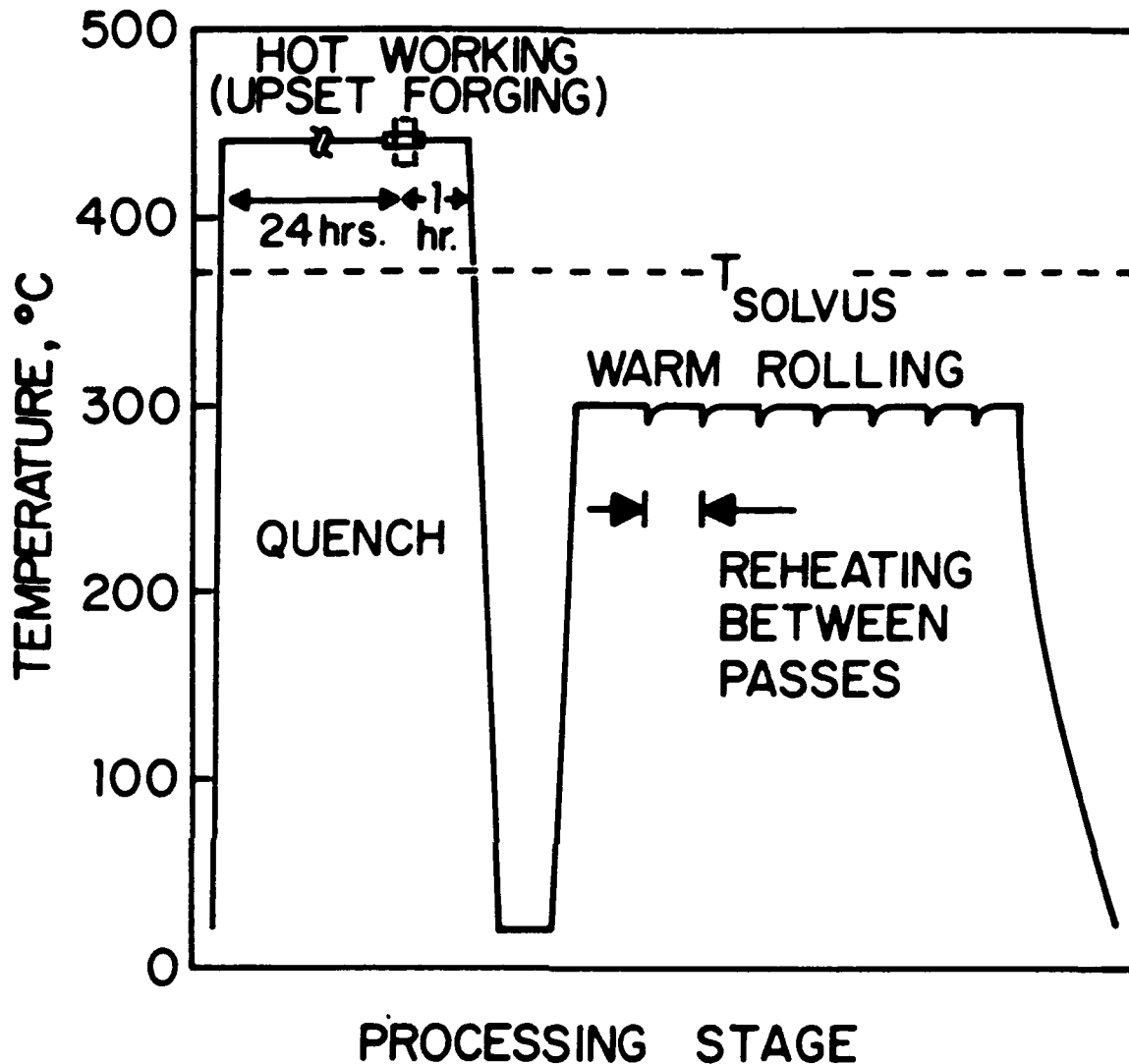
13

Figure 3.   General TMP Schematic

from above the soluvs temperature. Once the billets were thoroughly solution treated,

they were oil quenched for one minute and then cut in half transversely to facilitate

phase two of the TMP.

Phase two of the TMP consisted of warm rolling the billets at 300°C., a temperature

well below the β phase soluvs of 365°C. The billets were first heated at 300°C in a Blue

M electric box type furnace, model number 8655F-3, for 30 minutes. Furnace temperature was monitored by use of a type K (Chromel and Alumel) thermocouple attached to a digital readout (Newport Laboratory model number 267B-KCL). To maintain near isothermal conditions, a steel plate was placed under the specimens to act as a heat capacitor and the furnace temperature was monitored by measuring the temperature of the plate.

A Fenn Laboratory rolling mill with roll diameters of 4.0 inches, rotating at a rate of 0.327 rad/sec was used to perform the warm rolling. The rolling schedule for the TMP-8 processing schedule used in this work is summarized in Table 2. The desired mill gap was

Table 2. TMP-8 ROLLING SCHEDULE

| Pass	Mill Gap (in)	H_i (in)	H_f (in)	ΔH (in)	Mill Deflection (in)	True Strain ε (pct.)
1	0.838	1.024	0.869	0.155	0.031	15.14
2	0.742	0.869	0.774	0.095	0.032	10.9
3	0.657	0.774	0.684	0.090	0.117	11.6
4	0.581	0.686	0.614	0.072	0.105	10.5
5	0.506	0.614	0.536	0.078	0.108	12.7
6	0.431	0.536	0.463	0.073	0.032	13.6
7	0.338	0.463	0.387	0.076	0.049	16.4
8	0.227	0.387	0.265	0.112	0.038	31.5
9	0.112	0.265	0.159	0.106	0.037	40.0
10	0.043	0.159	0.092	0.049	0.067	42.2

set by hand using gage blocks, and taken to be accurate to within +/- 0.001 inches. The thickness was measured after each pass using a digital micrometer. The material received a 30 minute anneal between successive passes. Annealing time was taken as the time between successive passes as less then a minute elapsed when the sample was re-

moved from the furnace, rolled, measured, and returned. Following the tenth and final pass, the material was water quenched. The final thickness was measured following the quench. To minimize the complications of the friction associated with the changing mill-gap geometry in the final passes silicone spray lubricant was applied to the rolls prior to each of the last four passes.

Following the quench, one end of the specimen was sectioned for later microstructural analysis while the remainder was machined into tensile test coupons. The geometry of these coupons may be seen in Figure 4. The end which had been sectioned was further divided into five pieces, first in the transverse direction then in the longitudinal direction. Four were annealled for 30 minutes, 1 hour, 5 hours, and 20 hours, respectively. The fifth piece was maintained in the as-rolled condition. At the conclusion of each annealing treatment the specimens were water quenched for one minute.

C. MECHANICAL TESTING

An extensive series of elevated temperature tensile tests were performed using an Instron Model 6027 testing machine, equipped with a 2.0 kN load cell. To achieve the elevated temperature, a Marshall model 2232 clamshell furnace was used. Eight type-K thermocouples were placed along the tensile axis of the apparatus to evaluate the temperature profile. These thermocouples were placed with an approximate spacing of two inches measured from the testing cage base plate and continuing along the extension rod. One thermocouple was attached to each grip. Monitoring the temperature in this manner combined with adjustments to the top middle and bottom controllers of the furnace, resulted in an isothermal region 9.5 in (232.7 mm) in length about the test specimen, with temperature variations of no more then +/- 1.0°C with position and 2.0°C with time.

Figure 4. Tensile Test Coupon Geometry.
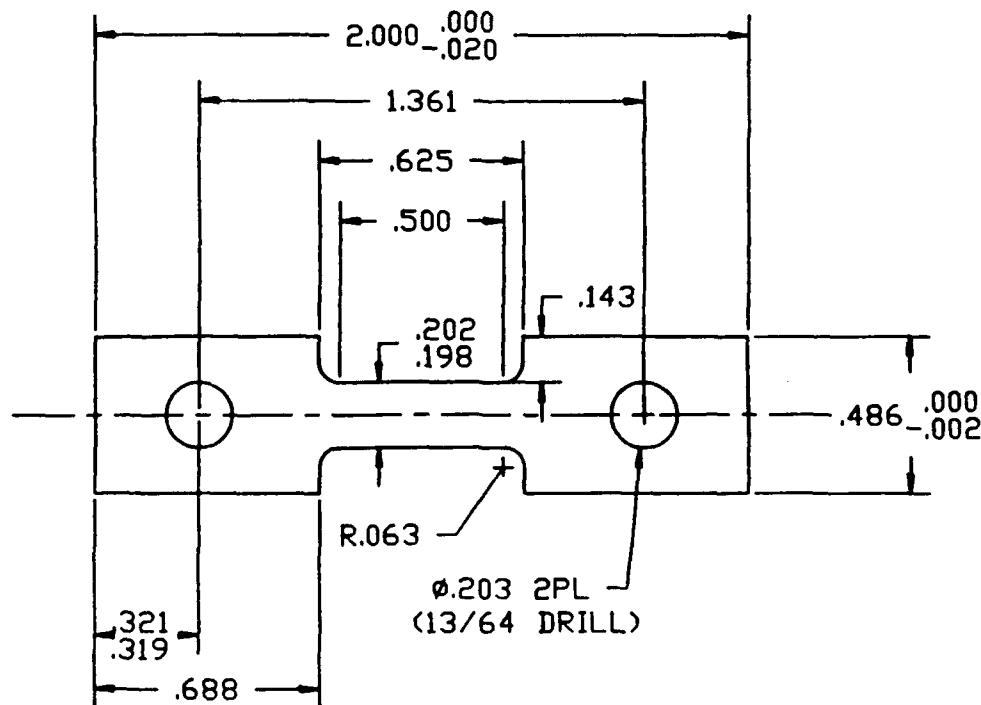
The testing coupons were placed in grips preheated to 150°C and then enclosed in the furnace which was maintained at 300°C. Coupons were allowed 43 minutes to come to temperature. Once at temperature, one of six separate constant cross head speeds was selected the resulting strain rates ranged from $6.414x10^{-5}$ sec^{-1} to $6.022x10^{-2}$ sec^{-1}. Each of these tests were conducted to failure. Tests were next conducted using strain rate of $6.46x10^{-5}$ sec^{-1} and $1.97x10^{-3}$ sec^{-1} to nominal true strain values of 0.10, 0.20, and 0.50.

D. DATA REDUCTION

For each test conducted, the following parameters were monitored: test time (mins), load (kN), displacement (mm), engineering stress (MPa), and engineering strain (pct.). From these data load vs. displacement curve was constructed. To account for any

17

elasticity slippage in the grips or compliance in the test assembly the corrected engineering stress as outlined by Lee and McNelley [Ref. 15] was first calculated and a plot of true stress vs. true strain then constructed. By first calculating the corrected engineering stress, σ_{corr}, data from all the test may be directly compared. Values of the true stress for true strains of 0.01, 0.02, 0.03, 0.05, 0.1, 0.2, and 0.5 were plotted versus strain rate on a double logarithmic axes to determine the strain dependence of the strain rate sensitivity coefficient m. The m-value was also assessed by performing a strain-rate cycling test where the cross head speed was cycled between 0.0508 mm/min and 0.1606 mm/min for every 5% increase in engineering strain.

E. SCANNING ELECTRON MICROSCOPY.

Backscatter imaging techniques were used to examine the microstructure and grain orientation of the as rolled, annealed, and tensile tested specimens. The backscattered imaging mode provided greater contrast than attainable using secondary electron imaging methods. Further explanation of this technique to enhance phase and orientation contrast is provided in [Ref. 14]

Each specimen to be examined was first sectioned to size using a low-speed diamond wheel, ground flat using successive 240, 320, 400, and 600 grit wet dry sand paper, and polished using 1.0 micron diamond paste such that the longitudinal-short (S-L) plane was prepared (Figure 5). The sample was then electropolished using a polishing solution of 10 pct. hydrochloric acid in 90 pct. 2-butoxyethanol. For polishing this solution was maintained at 0°C. A voltage of 14 VDC was applied for three, minutes resulting in an average current of 0.02 amps. The prepared samples were then mounted on viewing stage with the S-L planes in view using graphite cement. The specimens were viewed and studied in a Cambridge Model S200 scanning electron microscope equipped with a Tungsten filament and utilizing an accelerating potential of 20keV.
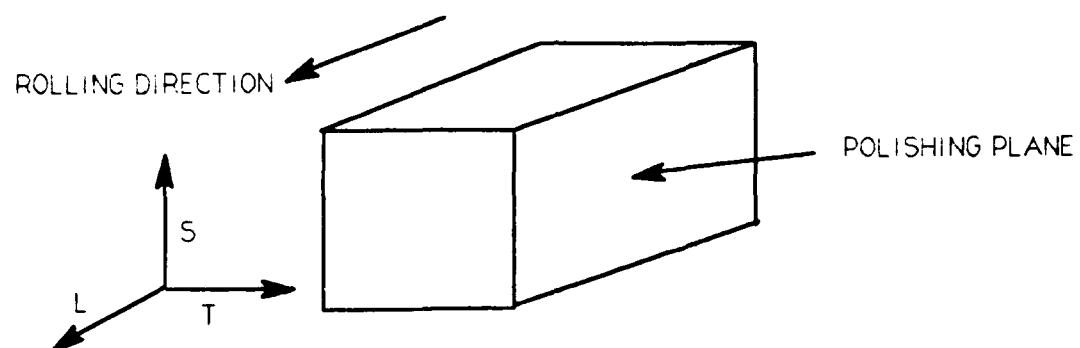
Figure 5.   Polishing Plane Geometry.

IV. RESULTS AND DISCUSSION

The PSN model for recrystallization of this alloy during interpass anneals of the TMP requires the precipitate particles to be of a greater size than the critical diameter for nucleation. This critical diameter depends, in turn, on the strain proceeding annealing. The study by Crooks, Kalu, and McNelley showed that PSN occurred upon annealing following the final pass and possibly during earlier passes as well. For this reason the straining history and especially the strain upon the last pass will determine the final grain size of the processed material. A larger strain on the final pass will correspond to a smaller critical particle size for PSN and this, in turn, will lead to more nucleation sites (assuming the size distribution of particles is the same). The resulting grain size of a material will be reduced if the number of nucleation sites is increased, and should enhance subsequent superplastic response.

Upon this basis the TMP6 schedule of Gorsuch [Ref. 17] was altered to provide a greater strain in the final pass while maintaining the same total strain. This was accomplished by decreasing the total number of rolling passes from 12 to 10, and by making smaller reductions in the initial passes. The strain in the final rolling pass was increased by a factor of two compared to the earlier work a still finer grain. The rolling schedules for the original TMP6 and for the TMP8 processes are shown in Figure 6 and Figure 7. The as-rolled microstructure of the material processes by TMP8 is shown in Figure 8. Deformation zones are present around the particles. A fine grain structure becomes apparent following 30 minutes of annealing at 300°C (Figure 9).

A. MECHANICAL TESTING RESULTS

The TMP8 material was pulled to failure in tension utilizing six different strain rates ranging from $6.11 \times 10^{-5} sec^{-1}$ to $6.02 \times 10^{-2} sec^{-1}$ (Figure 10). The results of these tests to
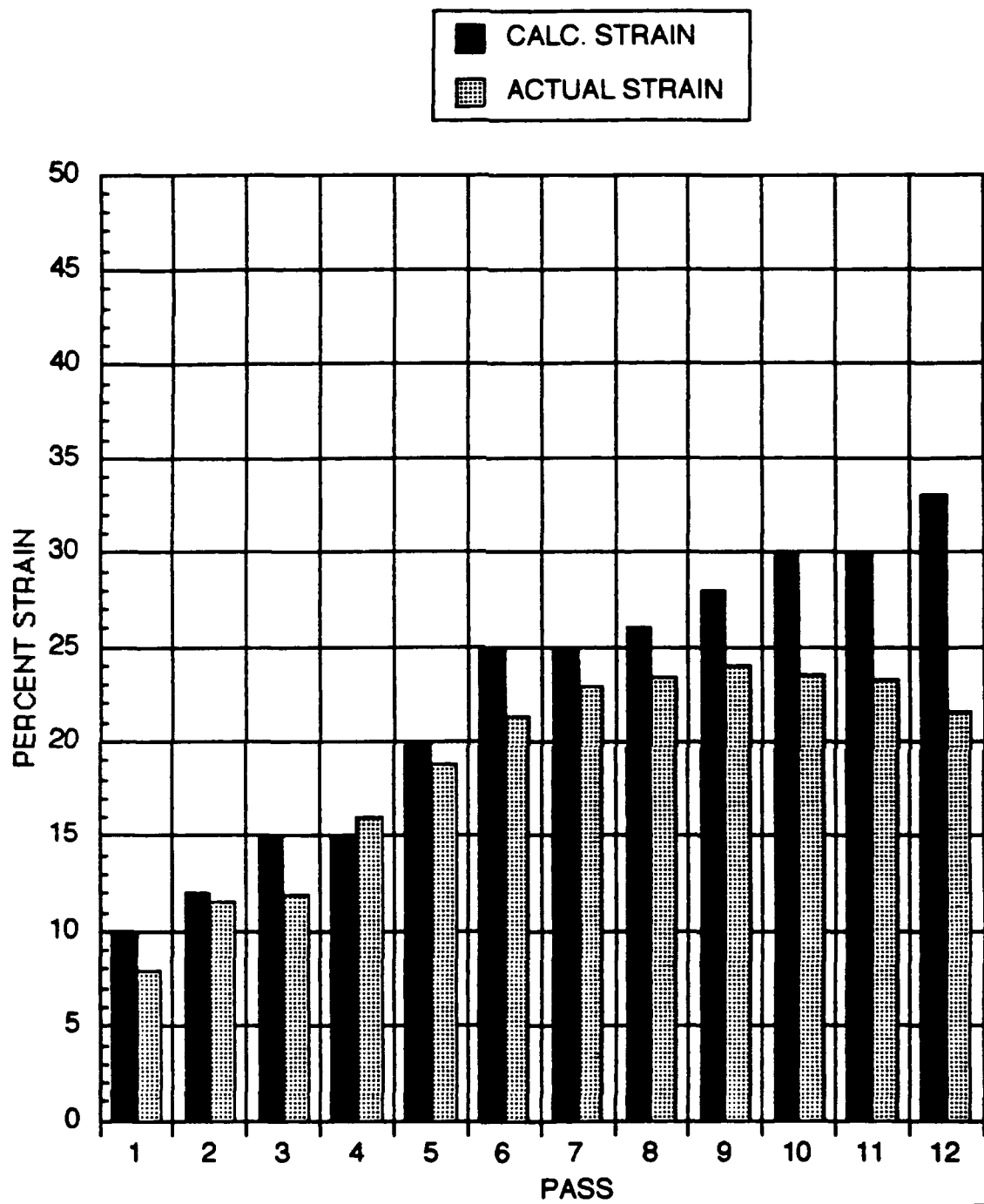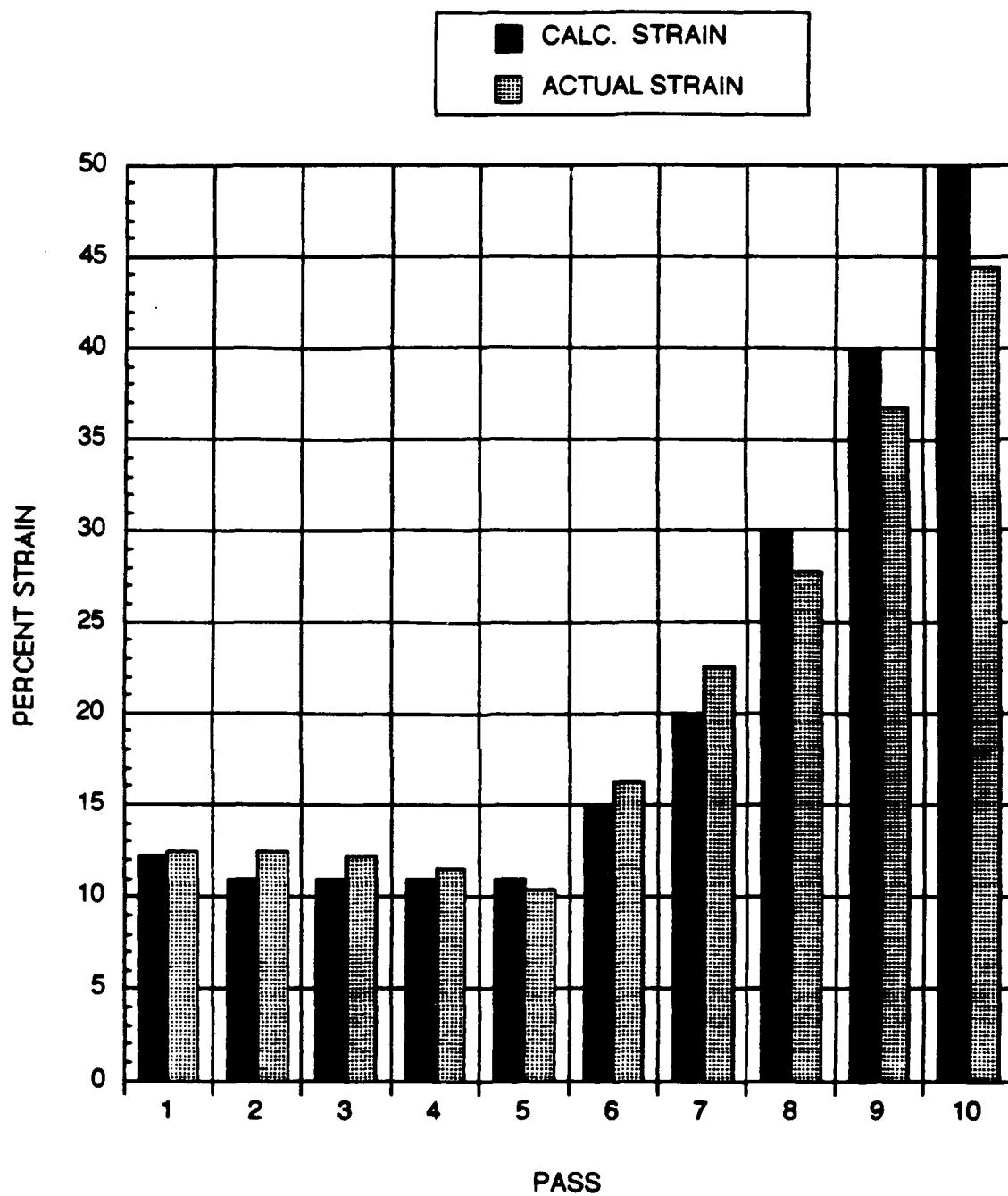
Figure 6. TMP6 Rolling Schedule
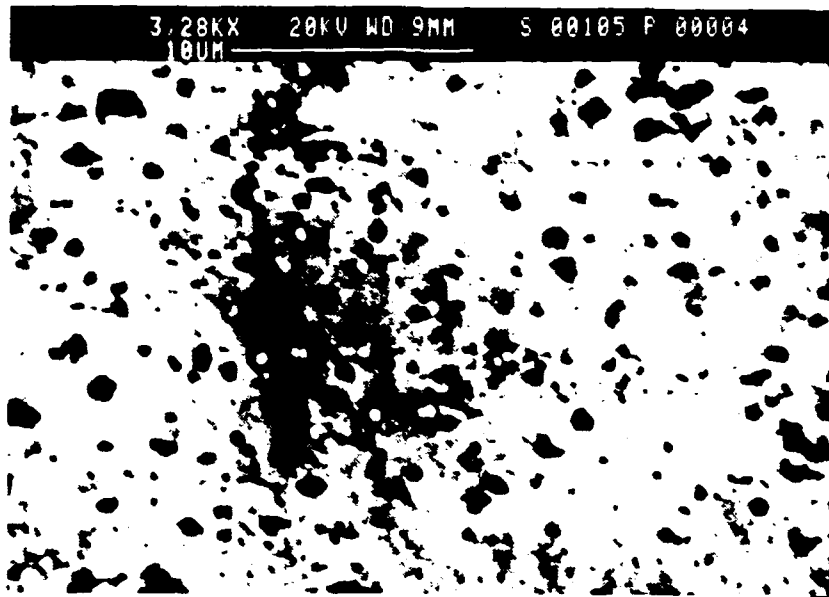
Figure 7. TMP8 Rolling Schedule

Figure 8.   Electron Micrograph of TMP8 Material in as-rolled Condition

failure were then compared to those obtained by Gorsuch over a similar range of strain rates (Figure 11). This comparison shows the TMP8 material to be stronger at all strain rates, especially at the higher rates. However, the TMP6 material strain hardened to a greater extent then the TMP8, material requiring more than 0.30 true strain to reach ultimate tensile strength. These results suggest that the TMP8 material has a coarser, not a finer microstructure.

The ductility of the TMP8 material was compared to that of the TMP6 material. Figure 12 and Figure 13 show ductility verses strain-rate plots corresponding to the stress-strain data presented earlier for both rolling schedules. As is clearly shown, the TMP8 material less uniformly less ductile then the TMP6 material; however, the peak ductility for both materials occurs at nearly the same strain rate. Further, the TMP8 curve closely follows the same general shape as that of the TMP6. Comparison of the
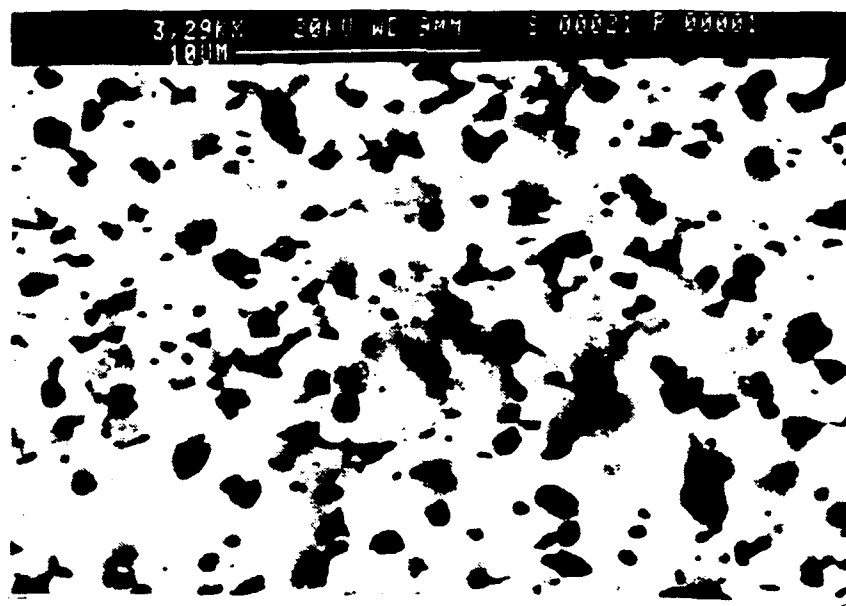
Figure 9. Electron Micrograph of TMP8 material following a 30 min. anneal

superplastic properties of the two processes again indicates the TMP-8 behaves as a coarser grained material then the TMP-6 material.

Figure 14 and Figure 15 directly compares the logσ verses log$\dot{\varepsilon}$ data for the TMP6 and TMP8 processes at true strains of 0.02 and 0.20. These plots were constructed from the stress-strain data presented earlier. The less ductile TMP8 material has a lower strain rate sensitivity coefficient value, m, than that of the TMP6 material. The lower value of m is consistent with a stronger, less ductile material. As shown in Figure 16, the strain rate sensitivity coefficients for both processing conditions decreases from higher values to a consistent value of m = 0.30. The TMP8 material decreases in m-value much more quickly then the TMP6 material, suggesting that the onset of deformation by dislocation motion occurs sooner in strain for the TMP8 material. Again, it would be expected on this basis that the TMP8 material will exhibit a lower ductility. Plots of logσ verses log$\dot{\varepsilon}$ at other strain values may be seen in appendix A.

24

will exhibit a lower ductility. Plots of $\log\sigma$ verses $\log\varepsilon$ at other strain values may be seen in appendix A.

B. ELECTRON MICROSCOPY

Scanning electron microscopy was utilized to examine microstructural evolution in the TMP8 material. Initial examination of the TMP8 material in the as-rolled and 300°C annealed conditions showed it to have comparable grain size and β particle size as the TMP6 material.

Scanning electron micrographs (backscattered imaging mode) were then obtained for specimens from tensile tests interrupted at nominal strains of 0.10, 0.2., and 0.50. These micrographs shown in Figure 17 through Figure 20 provide evidence of strain -enhanced grain growth. This may be seen in comparison of micrographs for grip and gage sections of the same sample. The grip and gage sections will have experienced the same time at temperature. Slight strains in the grip due to tightening are much smaller then the strains in the gage section. The grain sizes of these samples were measured for each of the interrupted test specimens and for a specimen which had been pulled to failure at the same strain rate. The results are shown in Figure 21. Deformation en-hanced grain growth during superplastic straining of Al-Mg alloys has been shown pre-viously and is present in addition to normal, static growth [Ref. 16]. Microstructural examination of the failed samples sections also demonstrated evidence of failure by grain boundary sliding which may be seen in Figure 22. At large strains, the β particles ap-pear to coalesce. This may also be seen at lower strains where the β phase, initially present in bands, begins to coalesce and form larger particles. As the grains begin to slide, The particles move closer to one another. When they become near enough, they combine to form a single large particle which is elongated in the direction of the grain boundary motion. Such growth and elongation of the β particles gives further evidence of deformation by grain boundary sliding.
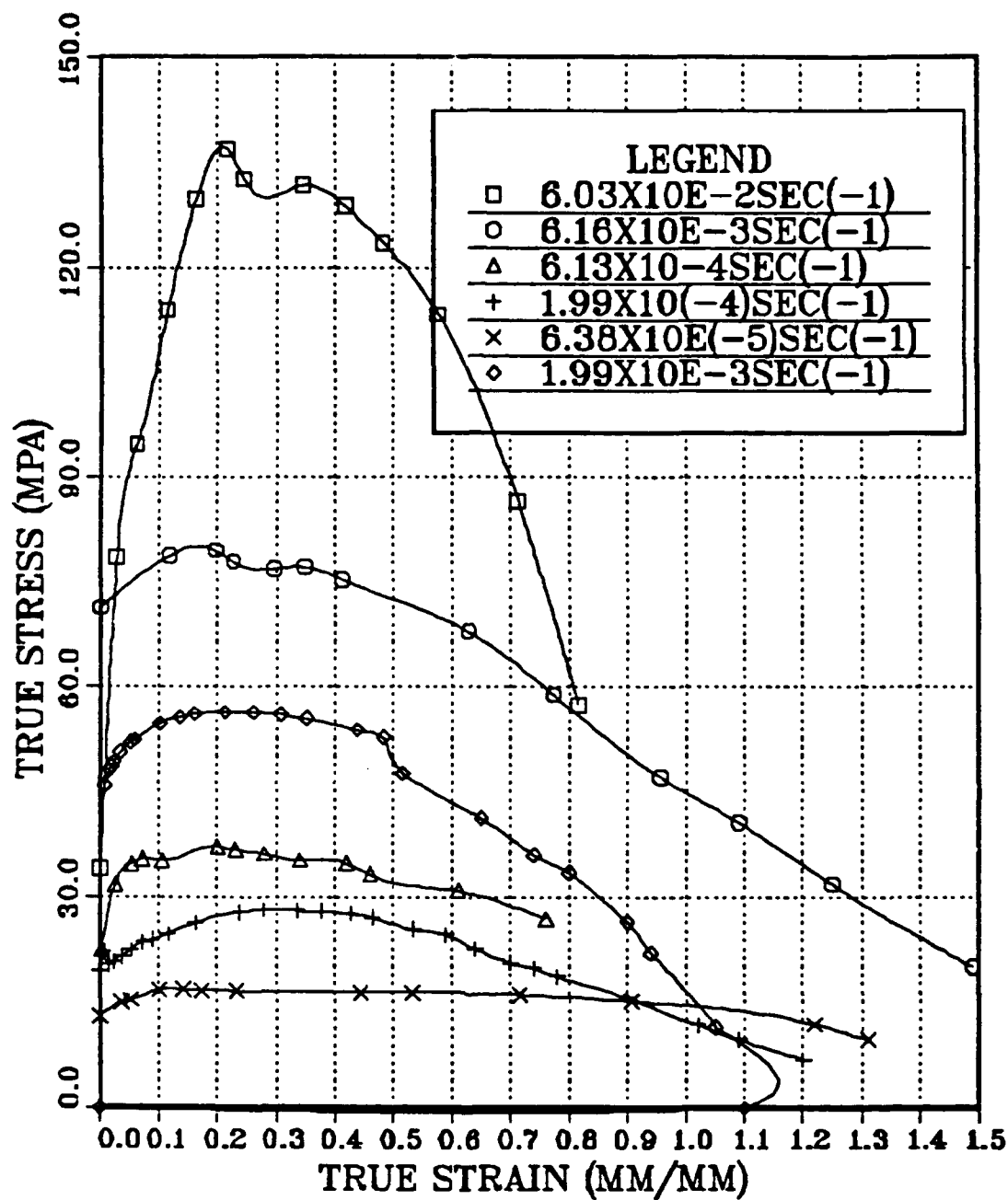
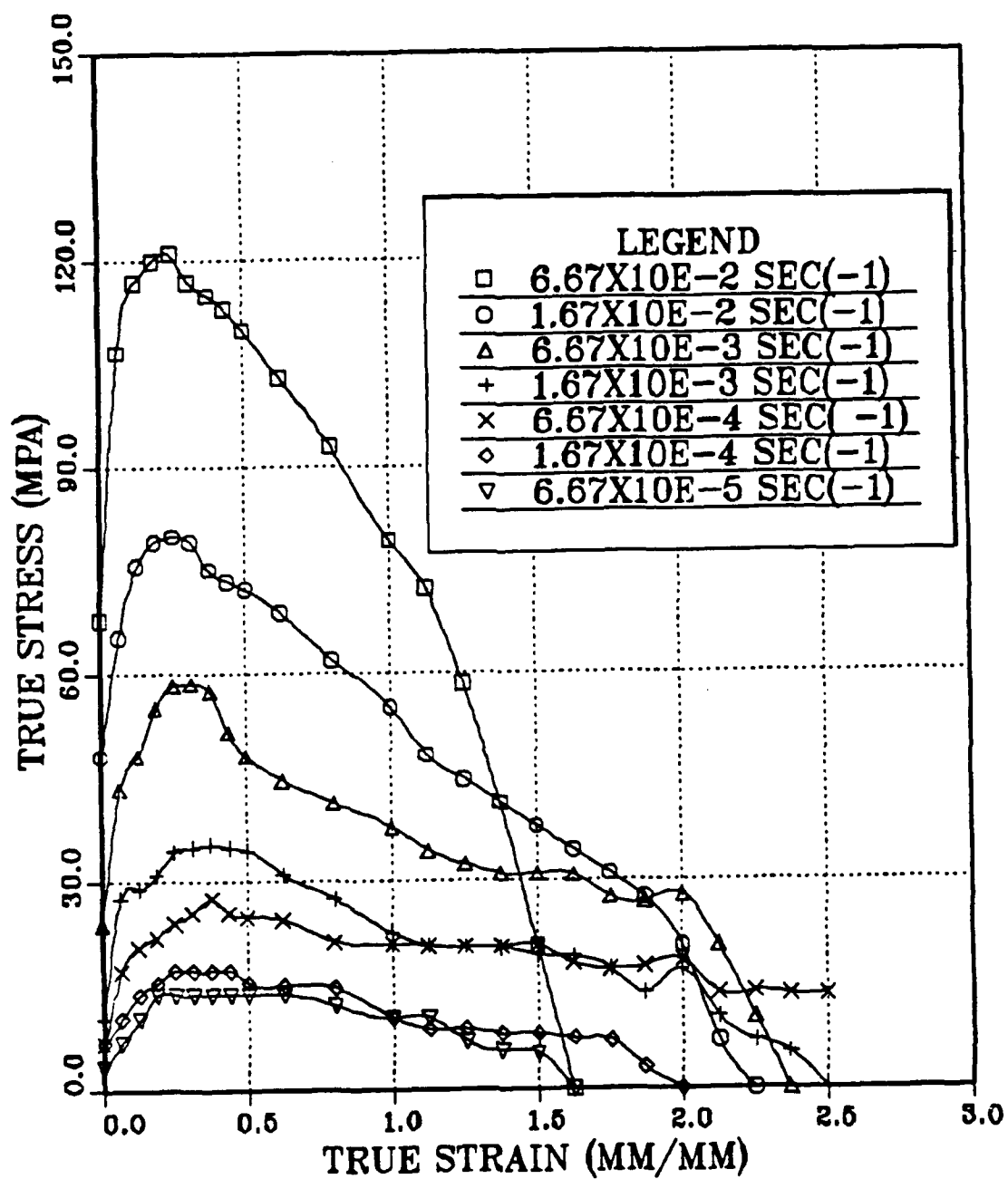Figure 10.   True Stress Strain Curve for TMP8

26
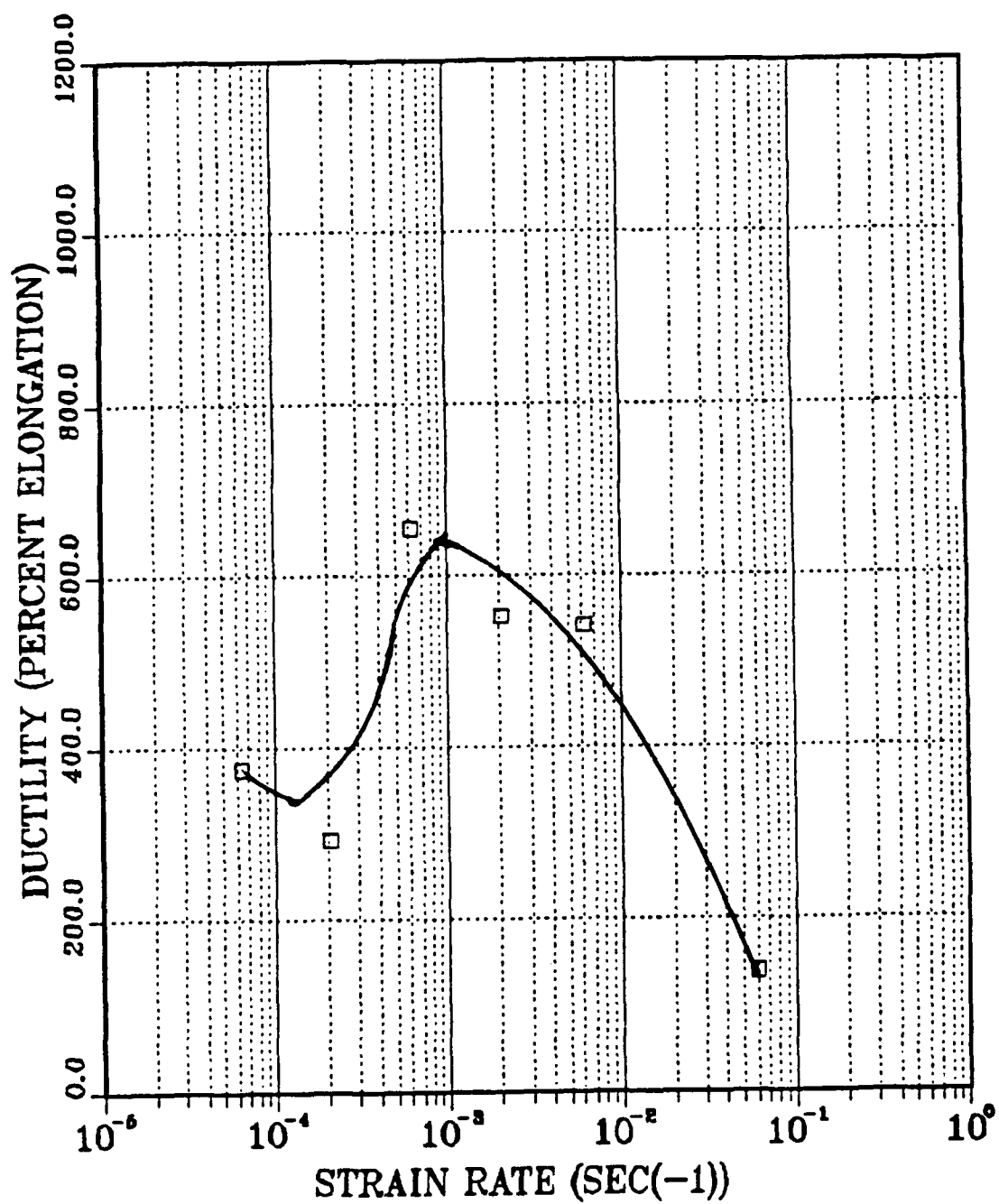
Figure 11. True Stress Strain Curves for TMP6

27

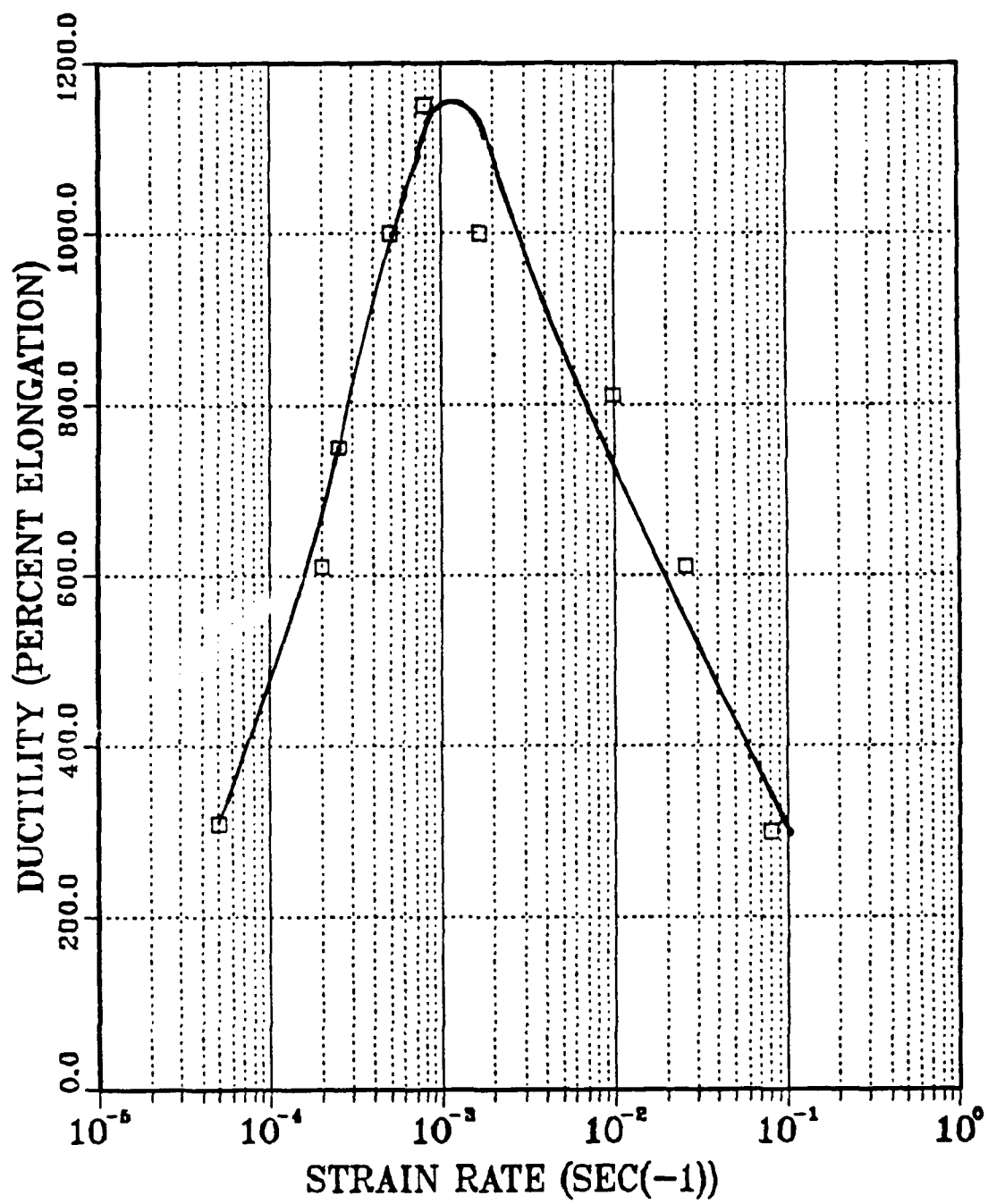Figure 12. Ductility vs. Strain Rate for TMP8

28

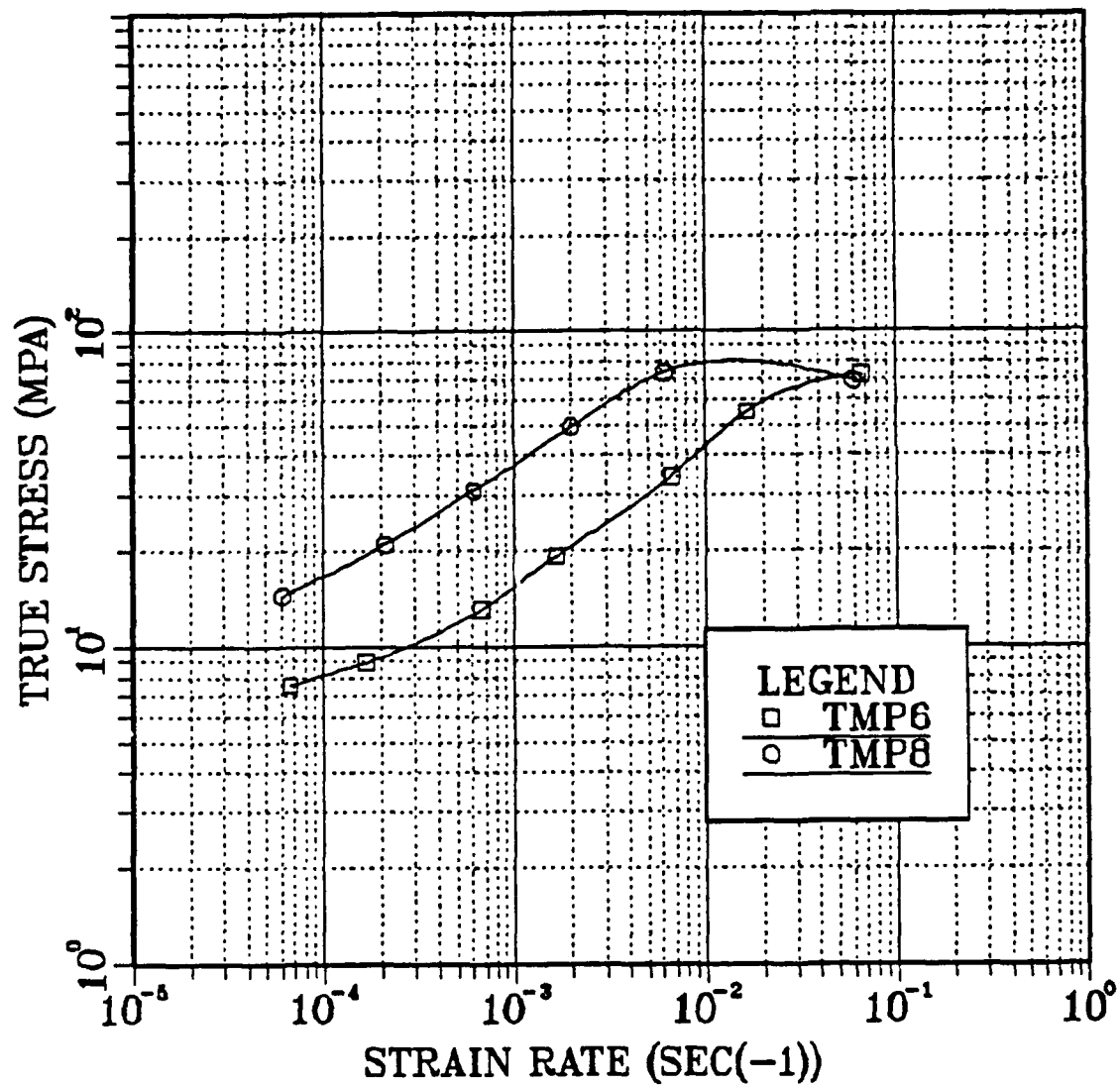Figure 13.   Ductility vs. Strain Rate for TMP6

29

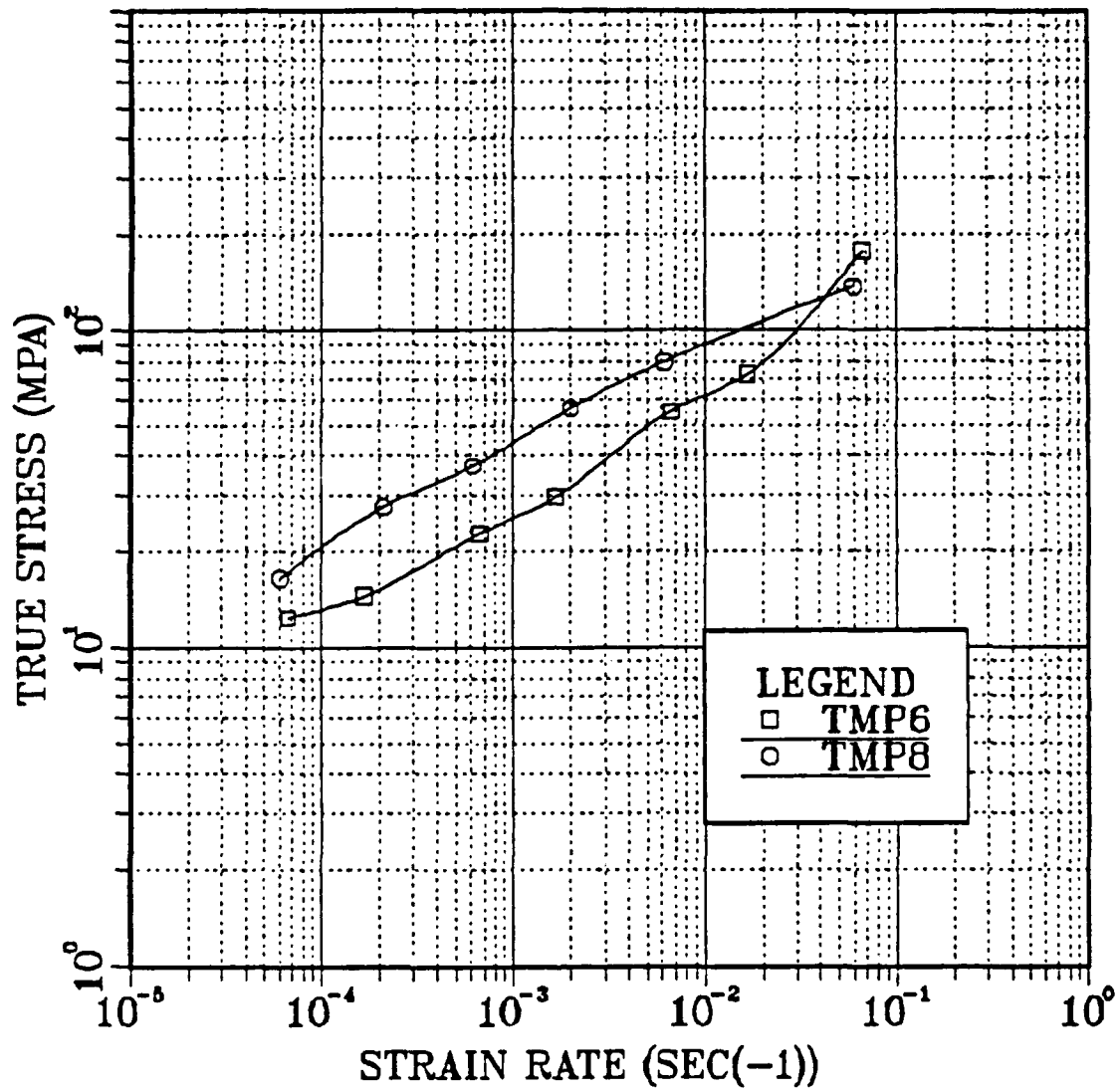Figure 14.   Strain Rate Sensitivity comparison at $\varepsilon = 0.02$

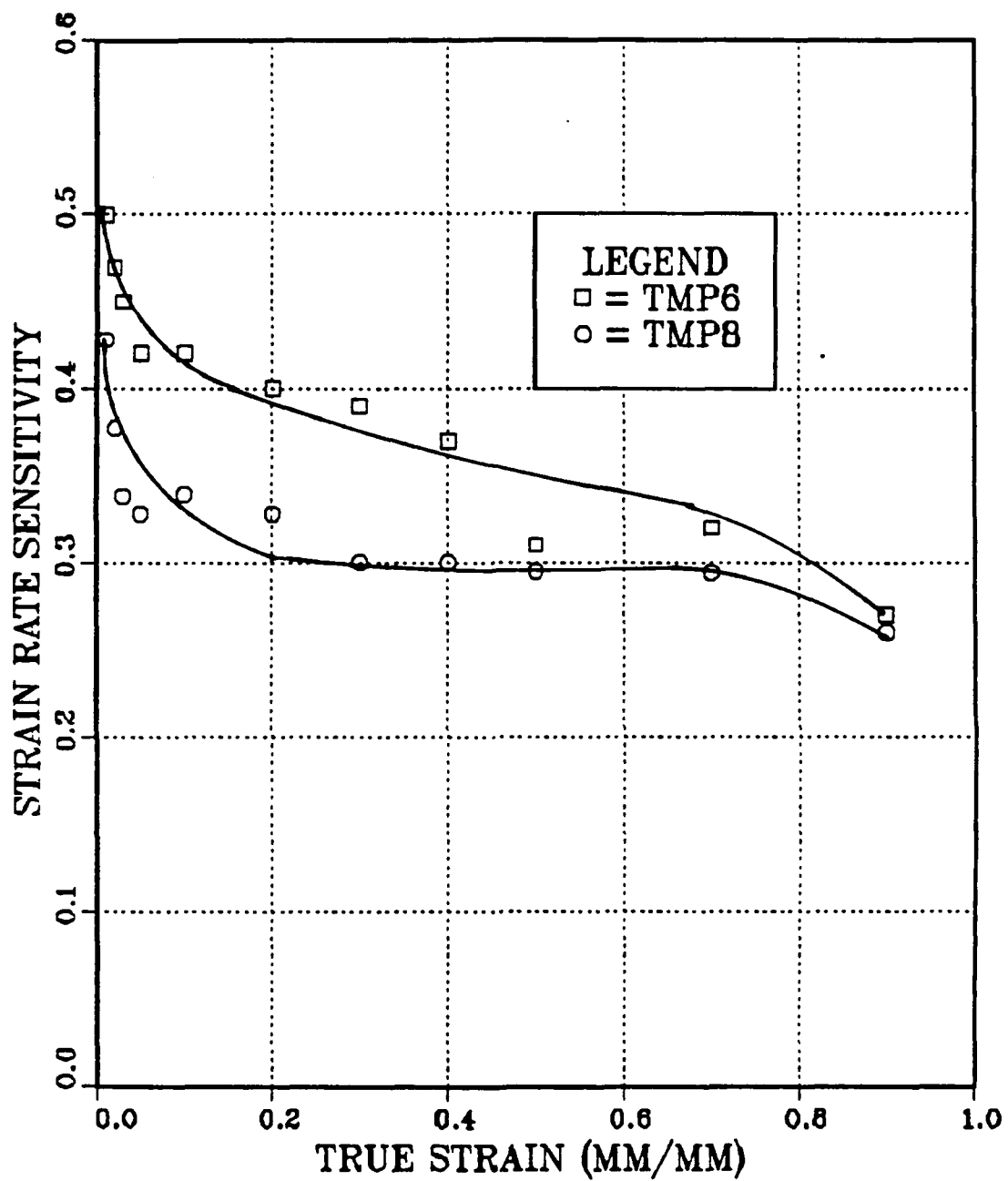Figure 15. Strain Rate Sensitivity comparison at $\varepsilon = 0.20$

Figure 16.   m vs. true strain for specimens pulled to failure

A final comparison of grain growth resulting during dynamic straining versus static annealing was conducted. The later samples for static annealing were heated in a furnace already at temperature and thus experienced a more rapid heating than those samples which had been placed in grips for tensile testing. Figure 23 shows the grains resulting from such static anneals are larger then those obtained due to the slower heating of the grip sections of mechanical test samples. The grain size is also relatively stable. This effect of heating rate was not studied further in this effort. Electron micrographs of the statically annealed samples may be seen in appendix B.

C. SUMMARY

To achieve superplastic deformation the microstructure of the material must be fine grained and stable with a homogeneous distribution of particles. By modifying the already successful TMP6 process such that a greater amount of strain was induced on the final pass, the TMP8 process was intended to result in a still-finer recrystallized grain size by particle stimulated nucleation at smaller β phase particles. The smaller critical particle size would result in a greater number of particles beyond the critical size required for nucleation and hence more nucleation sites would become active. The result would be recrystallization of the microstructure to an overall finer grain size (assuming nucleation site saturation). This finer grain size would result in a microstructure capable of greater superplastic deformation.

The microstructure resulting from the TMP8 process as evaluated by the mean linear intercept measurements proved to be nearly the same as that of the TMP6 process. Mechanical testing demonstrated the TMP8 material to be both stronger with less strain hardening and lower ductility than the TMP6 material, all which is indicative of a courser grained microstructure. A possible reason for this unexpected result is the assumption of site saturation limitation in the PSN recrystallization model. This model assumes there is instantaneous nucleation at time $t = 0$. Hence embryos form at all ac-
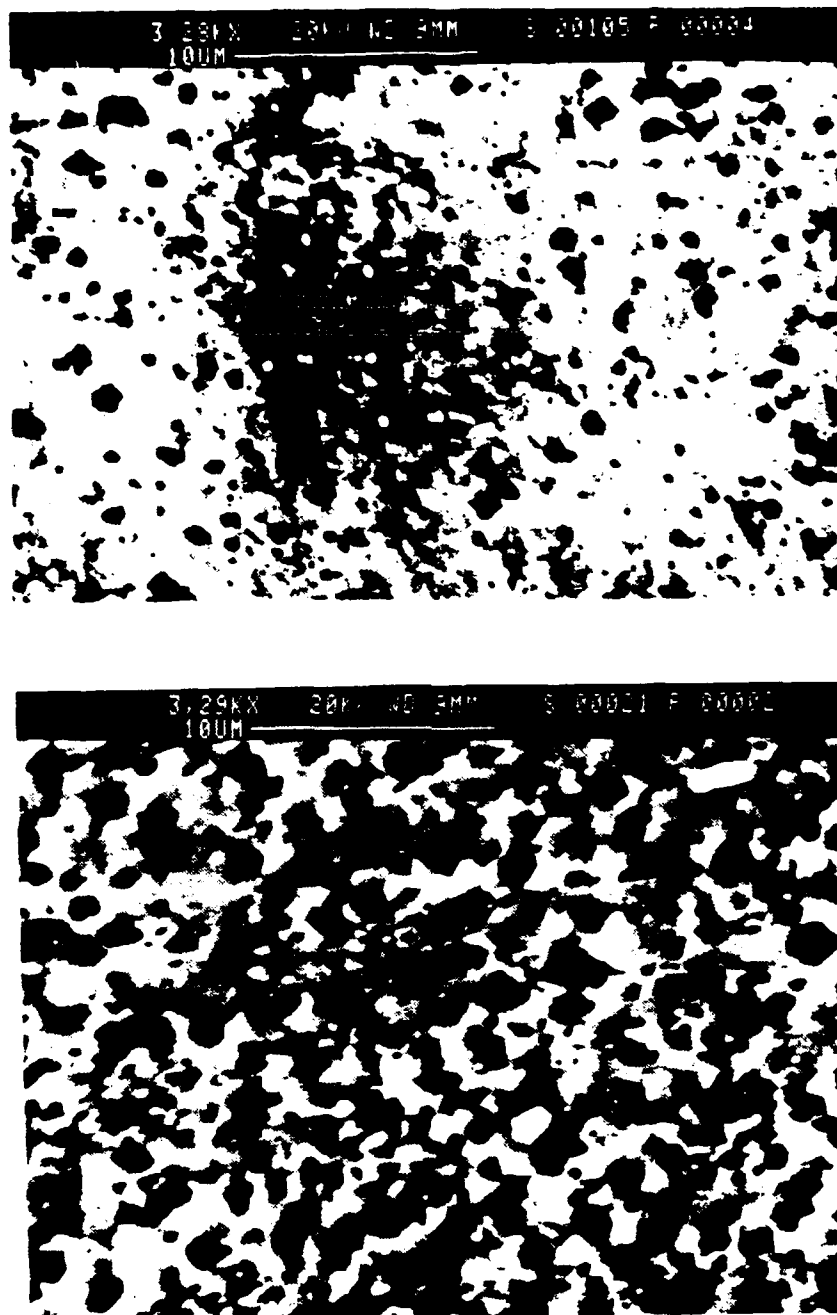
Figure 17. Electron Micrographs of TMP8 at $\dot{\varepsilon} = 6.11 \times 10^{-5} \text{sec}^{-1}$: Interrupted tensile test specimen at a strain of $\varepsilon = 0.134$. Grip section shown above, gage section below.
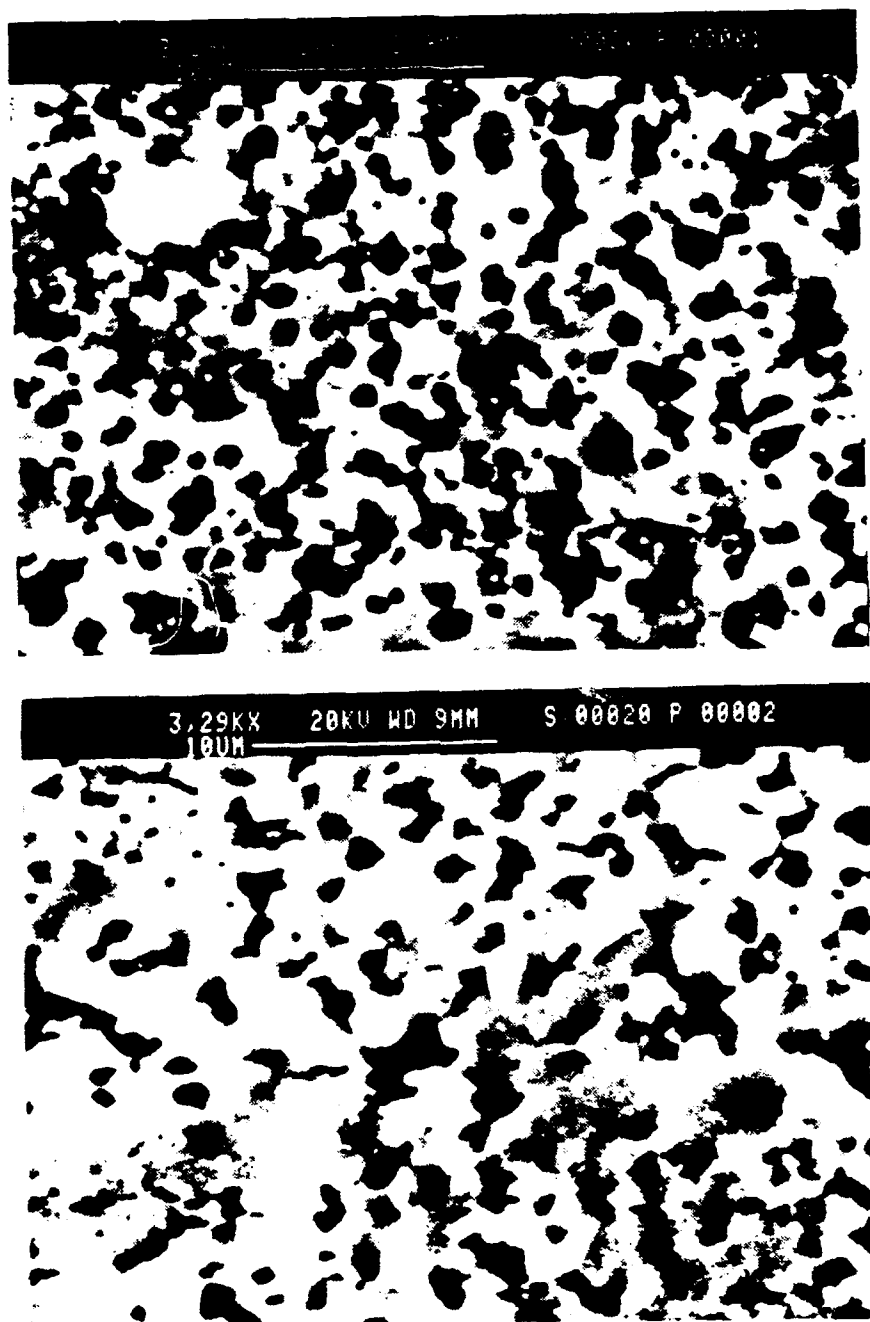
Figure 18. Electron Micrograph of TMP8 at $\dot{\varepsilon} = 6.11 \times 10^{-5} \text{sec}^{-1}$: Interrupted tensile test specimen at $\varepsilon = 0.379$. Grip section shown (above), gage section shown (below).
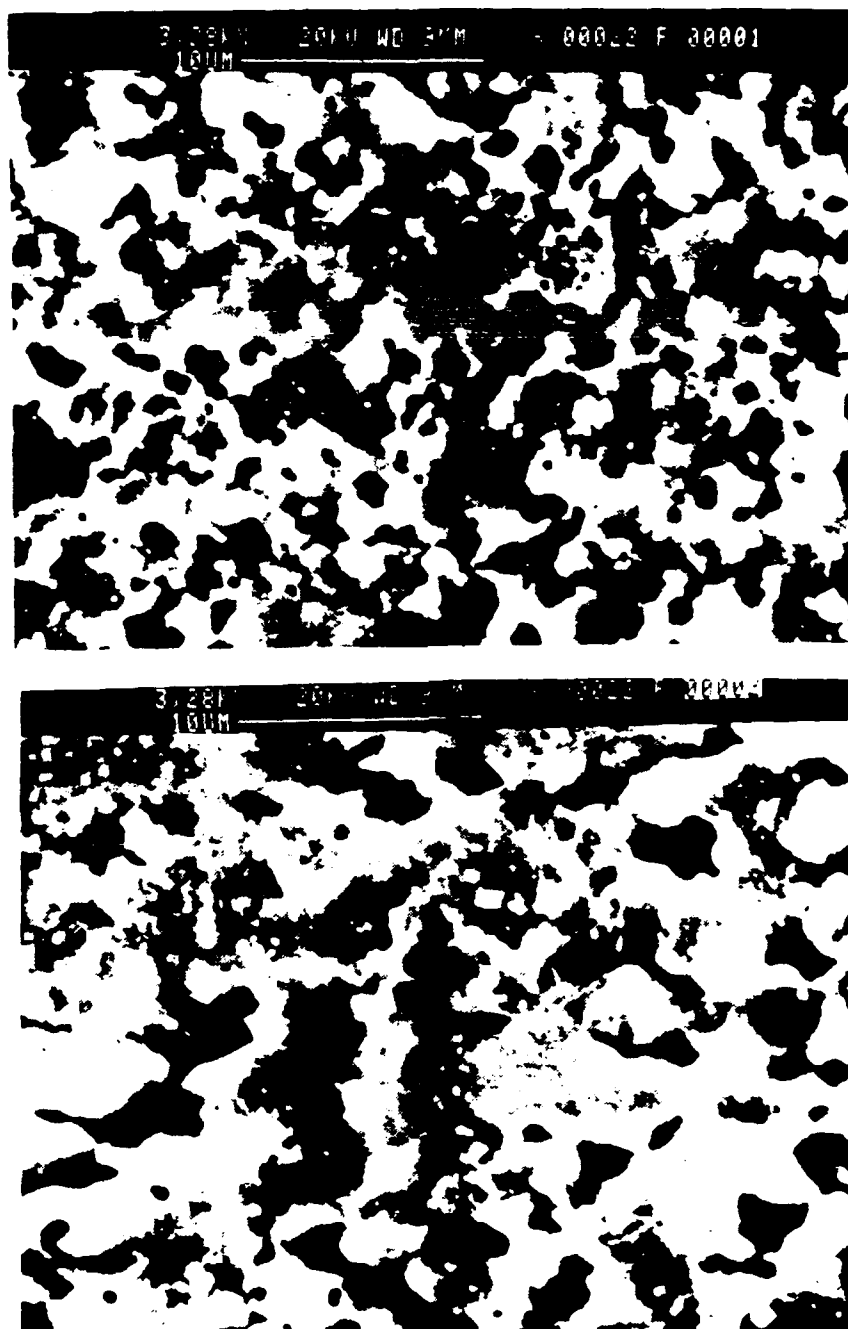
Figure 19. Electron Micrograph of TMP8 at $\varepsilon = 6.11 \times 10^{-5} \text{sec}^{-1}$.: Tensile specimen pulled to failure. Notice large difference in grain size in the grip section (above) and the gage section (below).
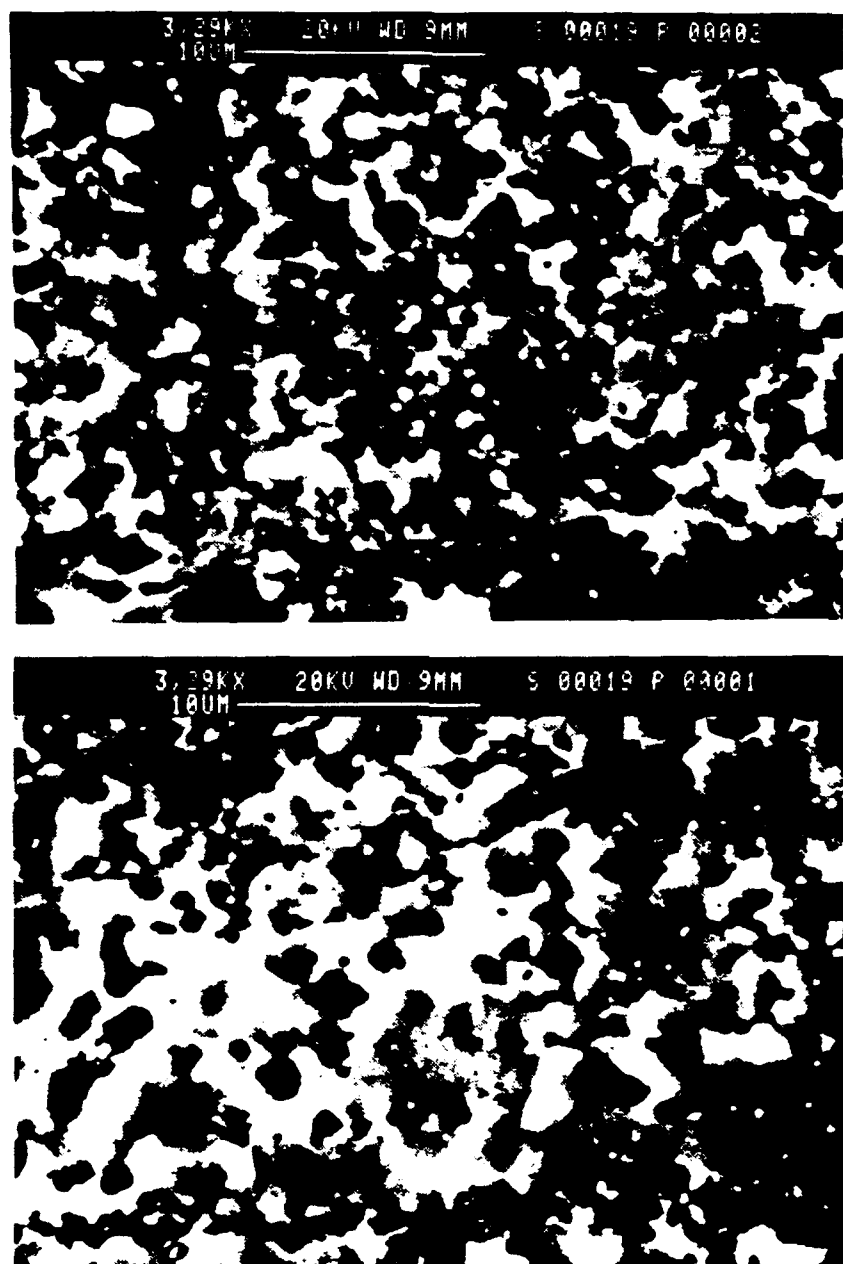
Figure 20.   Electron Micrographs of TMP8 at $\dot{\varepsilon} = 1.99\text{x}10^{-3}\text{sec}^{-1}$:   Interrupted tensile specimen showing relative grain growth of the grip section above and the gage section below at a higher strain rate then previously shown.
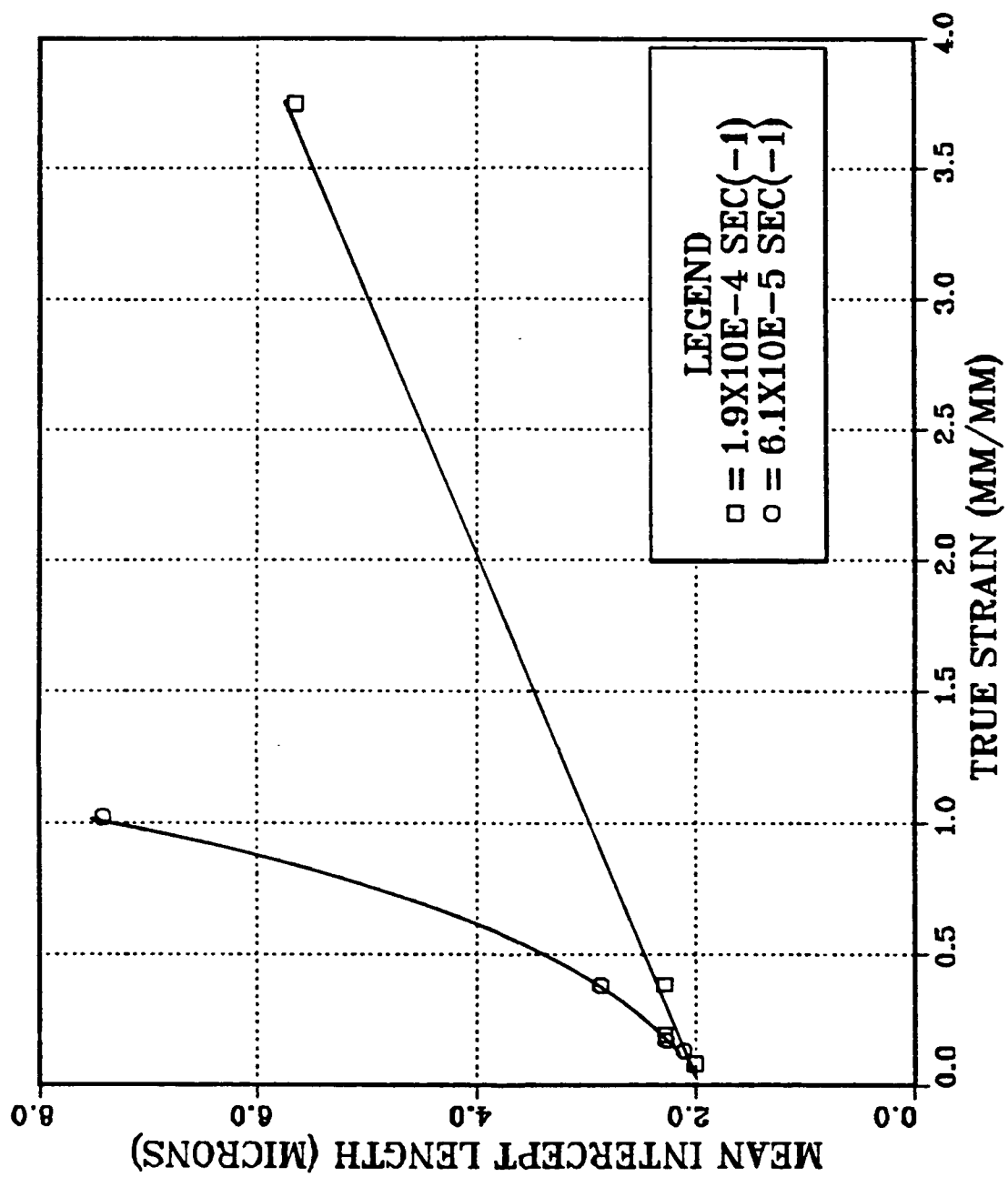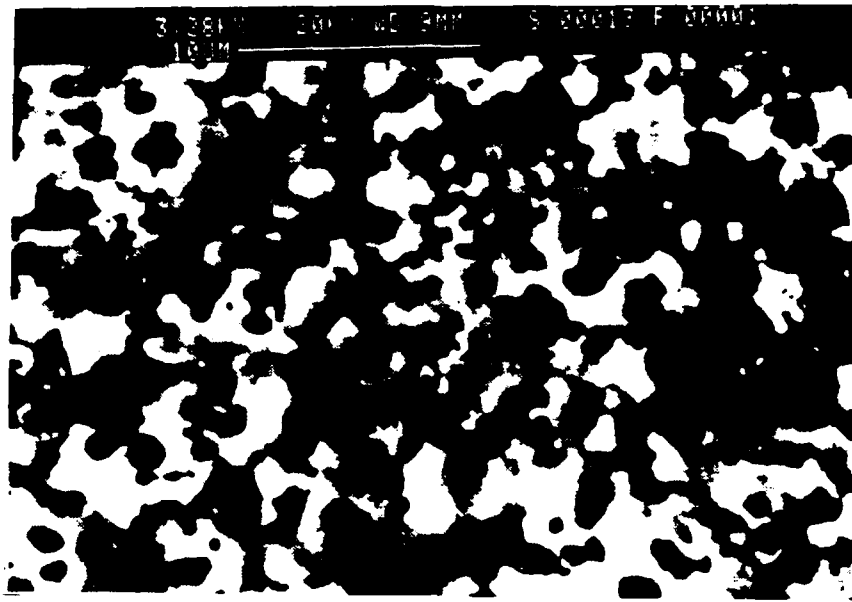
Figure 21. Grain Size vs. True Strain.

38

Figure 22. β Phase Coalescence at High Strain.

tive nucleation sites, than nucleate and grow but only until impinging on growing nuclei from adjacent nucleation sites. Thus the smaller the particle size required for nucleation, the finer the resulting recrystallized microstructure will be. If the model is relaxed to allow earlier nucleation at larger particles, the resulting grains would grow at the expense of the smaller grains as suggested by the Gibbs-Thompson relation [Ref. 19]. If this is the case, then the TMP8 process may have resulted in deformation zones sufficient for PSN at finer particles but the growth from adjacent particles prevented nucleation with the result a microstructure which is capable of superplastic deformation but with a grain size equal to or larger then that of the TMP6 process. This is consistent with the experimental data.

Scanning electron microscopy of specimens pulled to failure showed significant coarsening of the grains in the gage length as compared to those in the grip section. This coarsening was observed to be related to the strain rate, with the lower strain rates
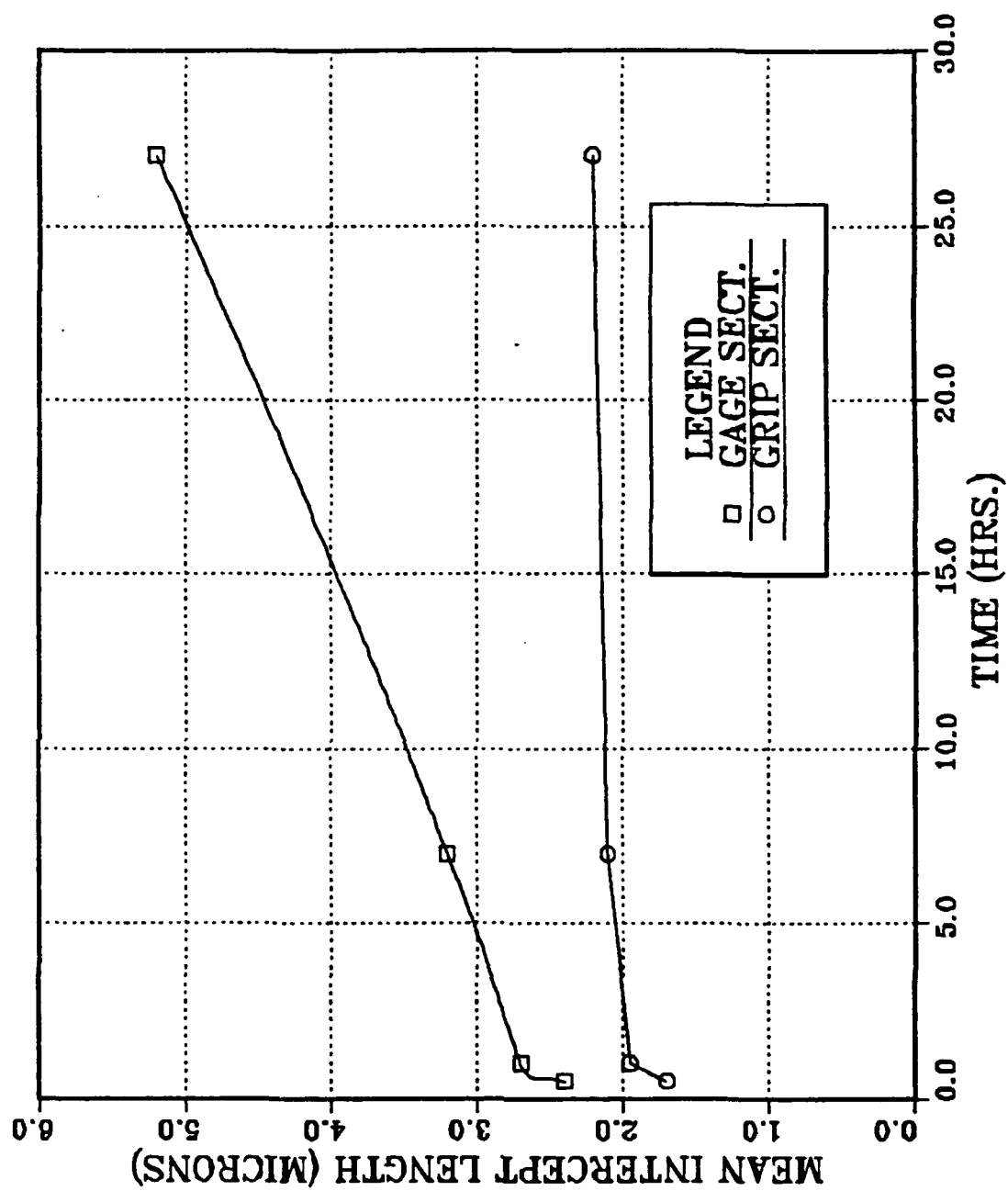
Figure 23.   Grain Size vs. Time at Temperature (300°C).

coarsening more extensively. However, when compared to statically annealed samples, the initial gage section grains were much smaller ($2\text{-}3\mu m$) and coarsened to a greater extent. This disparity in initial grain size may in part be due in some part to a higher heating rate experienced by the static annealed samples. Also noted in the gage sections of the heavily strained samples was significant coarsening of the β phase particles. The grains moving over the particles during deformation draw the particle closer together allowing them to coalesce giving further evidence of deformation by grain boundary sliding.

V. CONCLUSIONS

The conclusions and observations resulting from this research are as follows:

1. The Al-10Mg-0.1Zr alloy is capable of superplastic deformation.

2. Prior to deformation by superplastic flow, the material is in a fully recrystallized state.

3. Recrystallization of the material occurs by particle stimulated nucleation (PSN) associated with the β phase during processing.

4. The TMP6 and TMP8 processing schedules result in similar grain and particle size despite the larger final pass strain of the TMP8 processing schedule.

5. The resulting recrystallized grains are stable and will grow more readily when strained then those grains not subjected to strain.

VI. RECOMMENDATIONS

The following recommendations are made for further research and study:

1. Determine the effect of heating rate on grain growth.

2. Study further the proposed model for particle stimulated nucleation. Specifically, assess the requirement for instantaneous site saturation of the active nucleation sites at time $t = 0$.

3. Quantify the grain and particle size measurements for the TMP6 and TMP8 processed materials.

4. Process other aluminum alloys by the TMP8 schedule. Determine whether greater strain in the final processing pass results in greater grain ductility and finer recrystallized grain size.
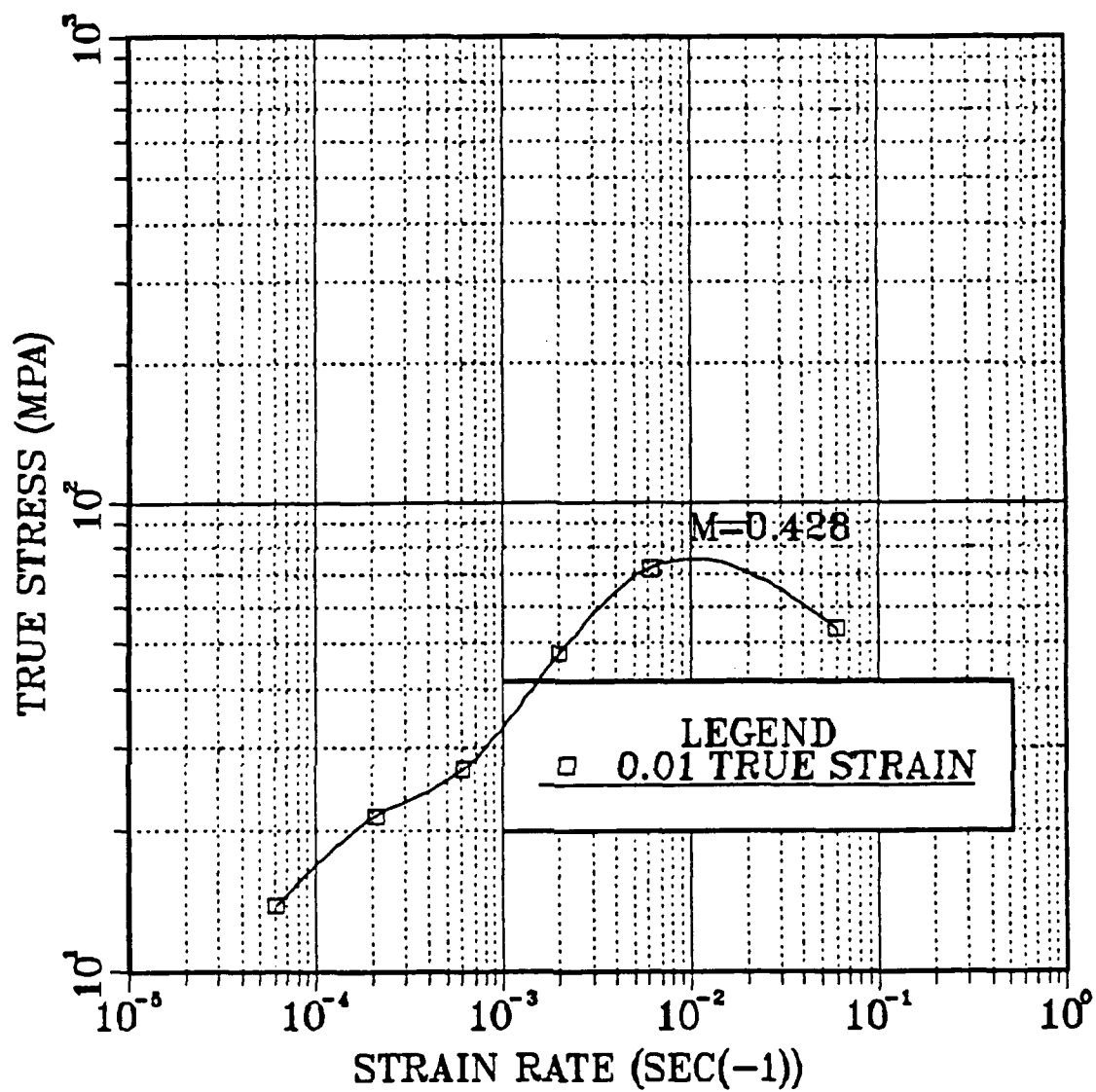
APPENDIX A. STRAIN RATE SENSITIVITY PLOTS

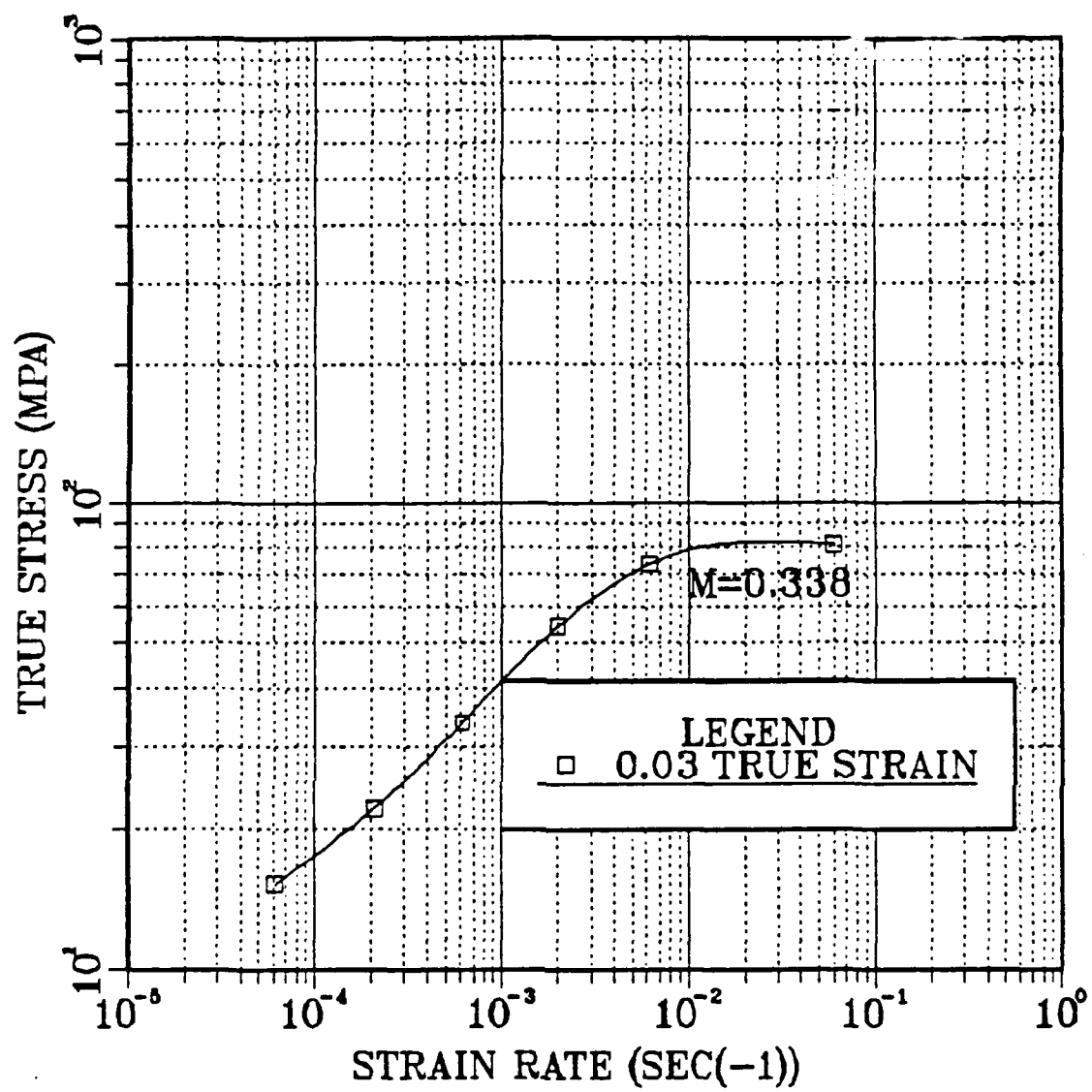Figure 24.   Strain rate sensitivity at $\varepsilon = 0.01$

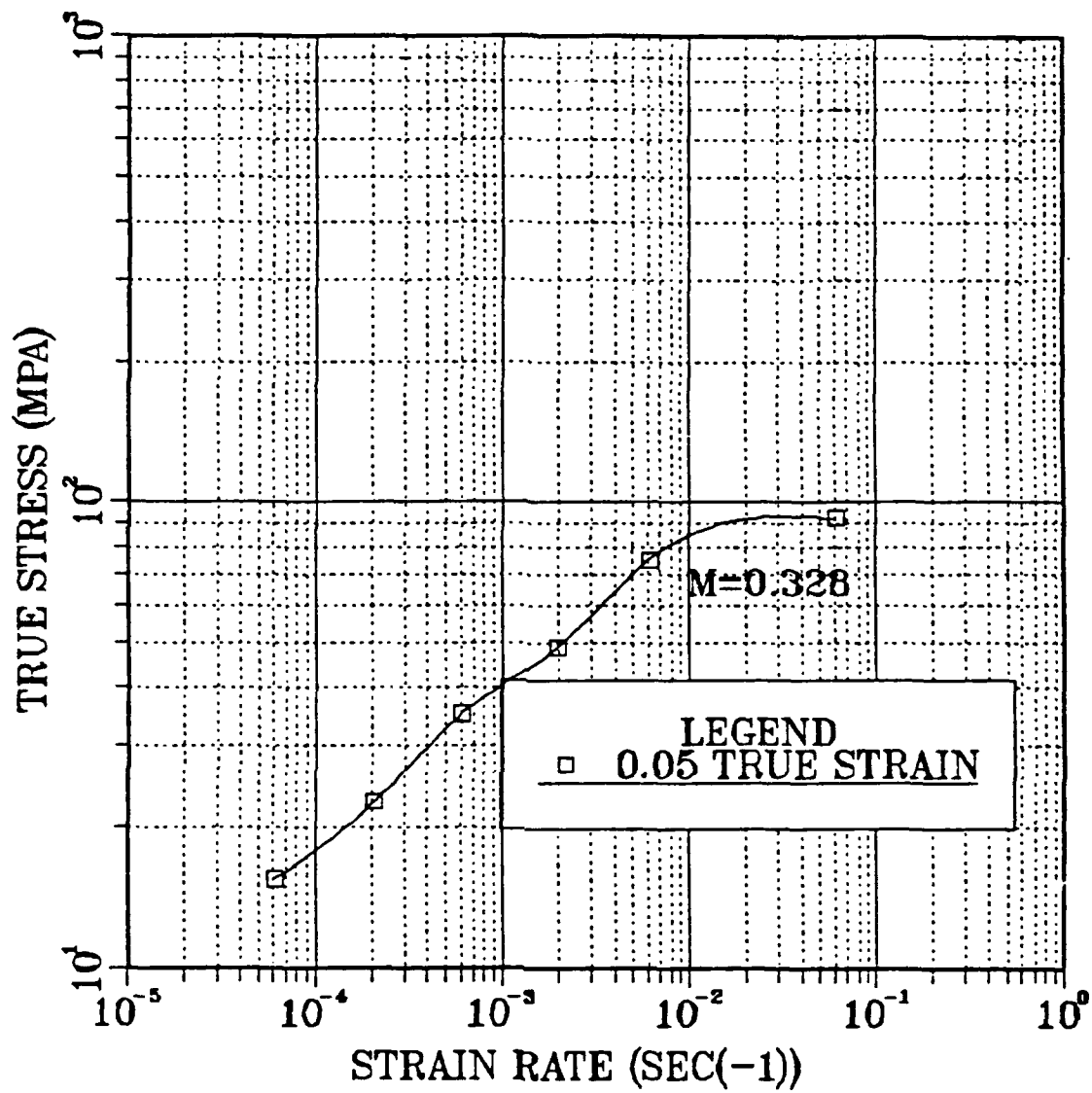Figure 25.   Strain rate sensitivity at $\varepsilon = 0.03$

Figure 26. Strain Rate Sensitivity at $\varepsilon \approx 0.05$
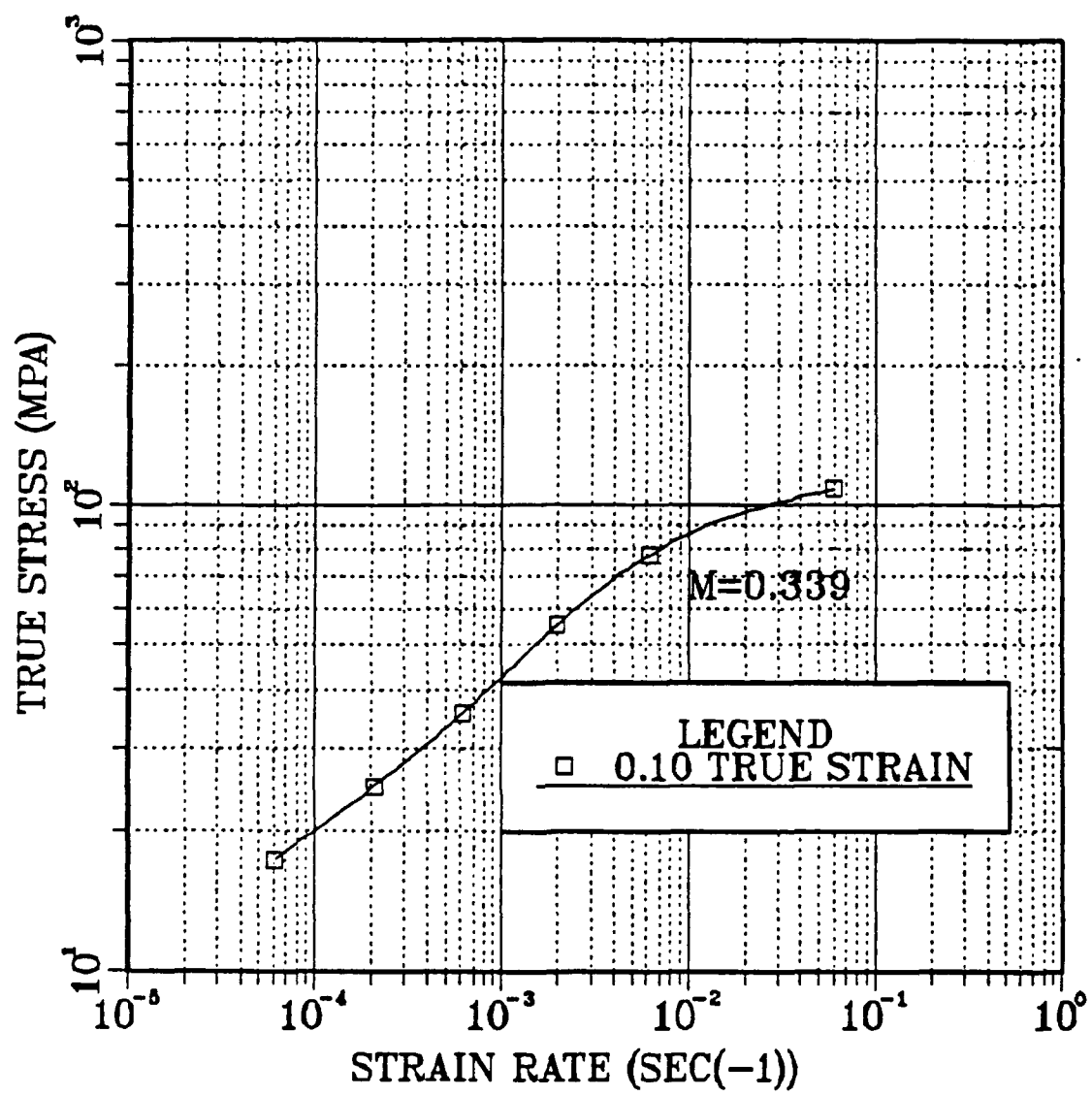
Figure 27. Strain rate sensitivity at $\varepsilon = 0.1$

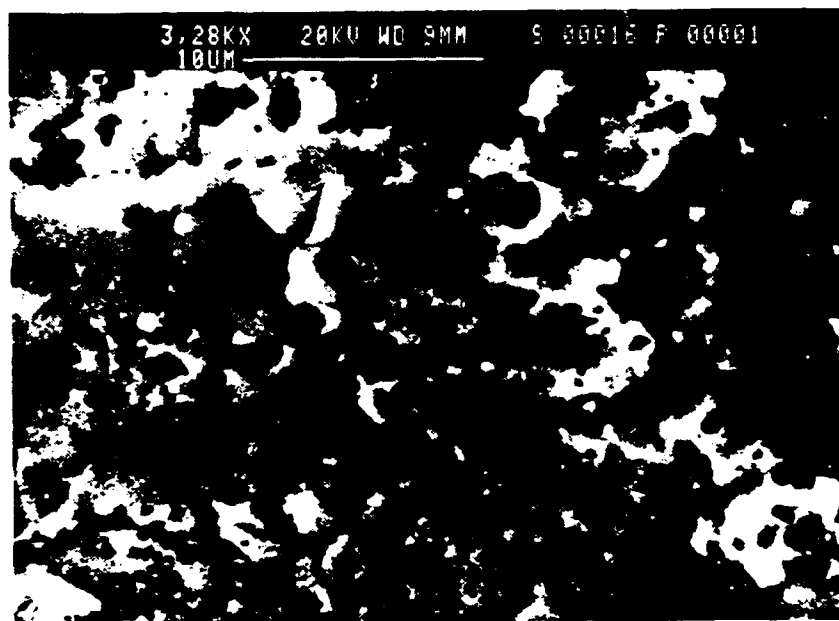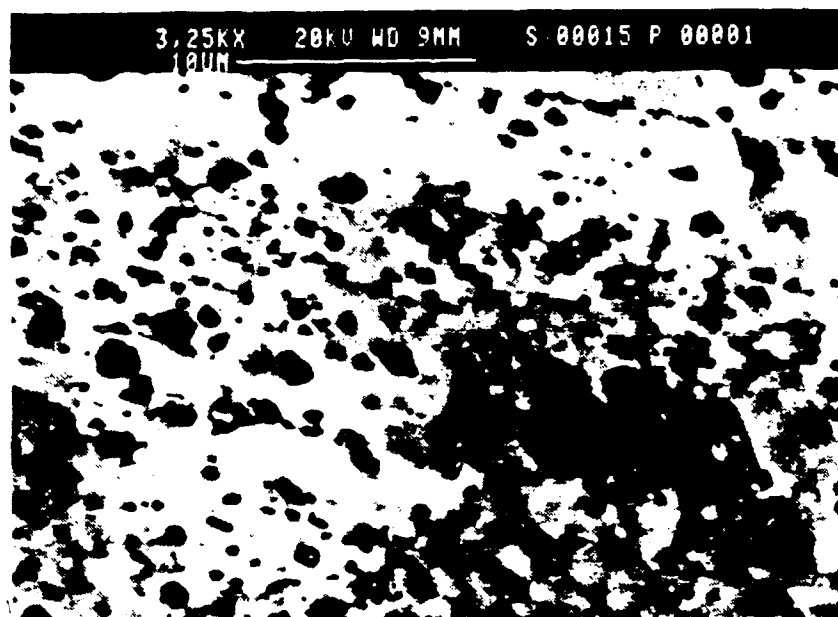# APPENDIX B. SCANNING ELECTRON MICROGRAPHS

Figure 28.   Micrographs of Statically Annealed TMP8:   Material annealed for 30
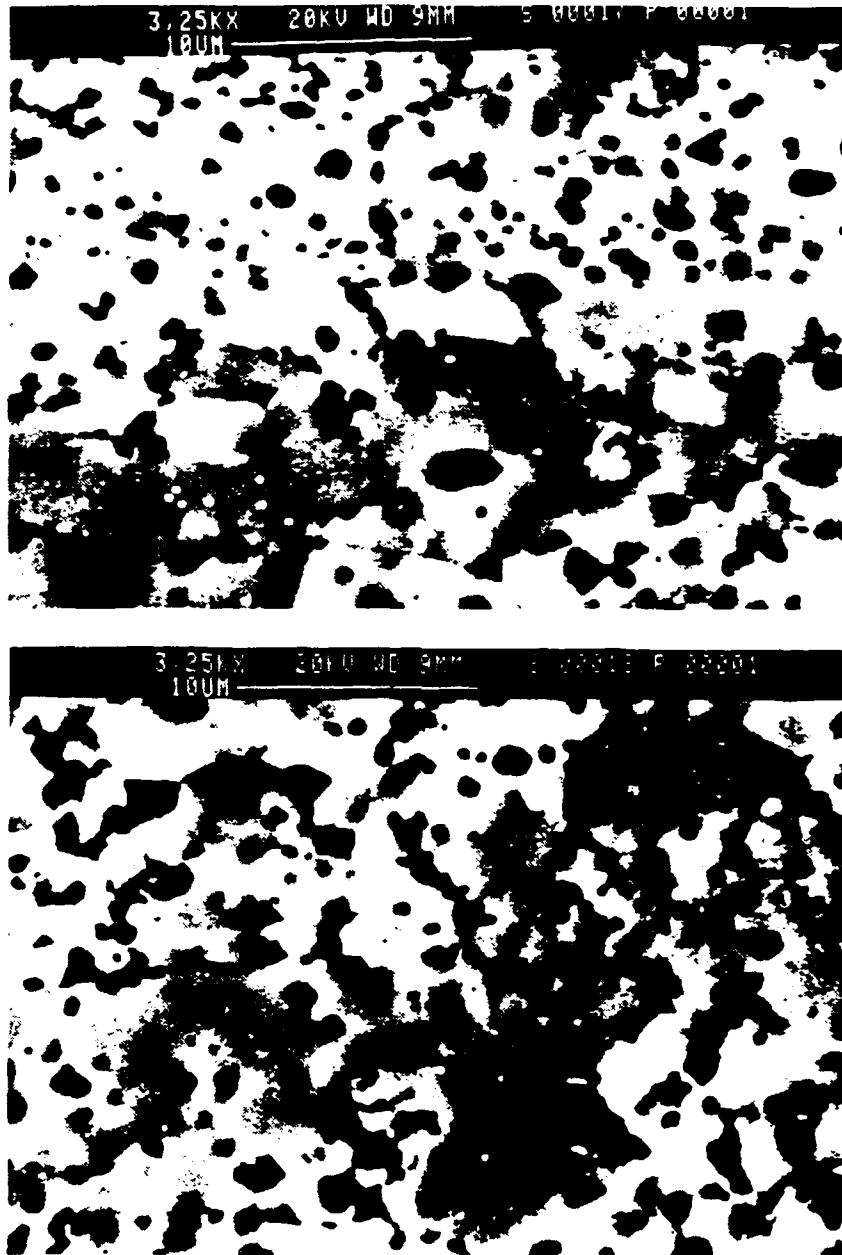minutes (above) and 1 hour below.

Figure 29. Micrographs of Statically Annealed TMP8: Material annealed for 5 hours (above) and 20 hours (below).

LIST OF REFERENCES

1. Sherby, O.D. and Wadsworth, J., "Development and Characterization of Fine-Grain Superplastic Materials," Deformation, Processing, and Structure, pp. 354-384, 1982.

2. Bengough, G.D. J. Inst. Metals, Vol. 7, 1912, p123.

3. Underwood, L.F., "A Review of Superplasticity and Related Phenomena," Journal of Metals, pp. 914-919, 1962.

4. Wakai, F., Kodama, Y., Murayama, N., Sakaguchi, S., Rouxel, T., Sato, S. and Nonami, T., "Superplasticity of Functional Ceramics," Superplasticity in Advanced Materials, ed. S. Hori, M. Tokizene and N. Furushiro, The Japan Society for Research on Superplasticity, pp. 205-214, 1991.

5. Wakai, F., Sakaguchi, S. and Matsuna, Y. Advanced Ceramic Materials, Vol. 1, p259, 1986.

6. Schey, J.A., Introduction to Manufacturing Processes, McGraw-Hill Book Company, 1977.

7. Buadelct, B., "Industrial Aspects of Superplasticity," Materials Science and Engineering, Vol. A137, pp.41-55, 1991.

8. Metals Handbook, Desk Edition, American Society for Metals, 1985.

9. Meyers, M.A. and Chawla, K.K., Mechanical Metallurgy Principles and Applications, Puntree-Hall Inc., 1984.

10. Askland, D.R., The Science and Engineering of Materials 2nd Ed., PWS-Kent, 1989.

11. Hales, S.J. and McNelley, T.R., "Microstructural Evolution by Continious Recrystallization in Superplastic Al-Mg Alloys," Acta Metallurgica, Vol. 36, No. 5, pp. 1229-1239, 1988.

12. Garg, A. and McNelley, T.R., "Development of Structure and Mechanical Properties in Al-10.2 wt. pct. Mg By Thermomechanical Processing," Scripta Metallurgica, Vol. 18, pp. 917-920.

13. Hales, S.J., McNelley, T.R. and McQueen, H.J., "Recrystallization and Superplasticity at 300°C in an Aluminum-Magnesium Alloy," Metallurgical Transactions, Vol. 22A, pp. 1037-1044, May 1991.

14. Crooks, R., Kalu, P.N. and McNelley, T.R., "Use of Backscattered Electron Imaging to Characterize Microstructures of a Superplastic Al-10Mg-0.1Zr Alloy," Scripta Metallufgica, Vol. 25, pp. 1321-1325, 1991.

15. Lee, E.W. and McNelley, T.R., "Microstructural Evolution During Processing and Superplastic Flow in a High Magnesium Al-Mg Alloy," <u>Materials Science and Engineering</u>, Vol. 93, pp. 45-55, 1987.

16. Hamilton, C.H., Ash, B.A., Sherwood, D. and Heikkinen, H.C., "Effect of Microstructural Dynamics on Superplasticity in Al Alloys," <u>Superplasticity in Aerospace</u>, ed. H.C. Heikkinen and T.R. McNelley, The Metallurgical Society, pp. 29-50, 1988.

17. <u>The Roles od Strain and Reheating Interval in Continious Recrystallization During the Thermomechanical Processing by Warm Rolling of an Al-Mg Alloy</u>, M.S. Thesis, Naval Postgraduate School, Monterey, California, December 1989.

18. Lyle, P.C., <u>Correlation of Processing, Microstructure, and Superplasticity in an Al-Mg-Zr Alloy</u>, M.S. Thesis, Naval Postgraduate School, Monterey, California, March 1992.

19. Shewmon, P.G., <u>Transformation in Metals</u>, McGraw-Hill, 1969.

INITIAL DISTRIBUTION LIST

		No. Copies
1.	Defense Technical Information Center Cameron Station Alexandria, VA 22304-6145	2
2.	Library, Code 52 Naval Postgraduate School Monterey, CA 93943-5002	2
3.	Naval Engineering Curricular Office Code 34 Naval Postgraduate School Monterey, CA 93943	1
4.	Professor T.R. McNelley, Code ME Mc Department of Mechanical Engineering Naval Postgraduate School Monterey, CA 93943	4
5	Adjunct Professor Peter N. Kalu, Code ME Ka Department of Mechanical Engineering Naval Postgraduate School Monterey, CA 93943	1
6.	Adjunct Professor R. Crooks, Code ME Mc Department of Mechanical Engineering Naval Postgraduate School Monterey, CA 93943	1
7.	Dr. Lesis Sloter, Code AIR 931A Headquarters, Naval Air Systems Command Washington D.C. 20361	1
8.	LT James F. Buckley II USN 2171 Idlewild Dr. Richland, MI 49083	2